

Advanced Energy Harvesters and Energy Storage for Powering Wearable and Implantable Medical Devices

Ziyan Gao, Yang Zhou, Jin Zhang, Javad Foroughi, Shuhua Peng, Ray H. Baughman, Zhong Lin Wang, and Chun H. Wang*

Wearable and implantable active medical devices (WIMDs) are transformative solutions for improving healthcare, offering continuous health monitoring, early disease detection, targeted treatments, personalized medicine, and connected health capabilities. Commercialized WIMDs use primary or rechargeable batteries to power their sensing, actuation, stimulation, and communication functions, and periodic battery replacements of implanted active medical devices pose major risks of surgical infections or inconvenience to users. Addressing the energy source challenge is critical for meeting the growing demand of the WIMD market that is reaching valuations in the tens of billions of dollars. This review critically assesses the recent advances in energy harvesting and storage technologies that can potentially eliminate the need for battery replacements. With a key focus on advanced materials that can enable energy harvesters to meet the energy needs of WIMDs, this review examines the crucial roles of advanced materials in improving the efficiencies of energy harvesters, wireless charging, and energy storage devices. This review concludes by highlighting the key challenges and opportunities in advanced materials necessary to achieve the vision of self-powered wearable and implantable active medical devices, eliminating the risks associated with surgical battery replacement and the inconvenience of frequent manual recharging.

1. Introduction

Commercialized active wearable and implantable active medical devices, denoted as WIMDs, represent a ground-breaking advancement in modern healthcare. These active devices, which rely on batteries for operation, can be worn on or implanted into the body. Integrating sensors, actuators, energy source, data capture and storage, communication microelectronic components, WIMDs enable a wide range of functionalities, from continuous monitoring to electromechanical actuation and nerve stimulation, catalyzing a transformative shift in healthcare delivery on a global scale. They have brought about significant benefits, including early detection and diagnosis of illnesses,^[1-3] targeted therapeutic interventions for effective management of chronic diseases^[4] and life-saving treatments,^[5] personalized rehabilitation,^[6,7] connected health,^[8] to name just a few. In addition, the realm of wearable medical devices has expanded beyond diagnosing and monitoring cardiac health to predicting heart failure well before its actual occurrence.^[9] For instance, Shi et al. have demonstrated an innovative fiber Bragg grating (FBG)-based

wearable sensor that enables precise and concurrent monitoring of respiratory and cardiac functions.^[10] More recently, digital and artificial intelligence technologies are increasingly being integrated into WIMDs for real-time decision making, further enhancing their capabilities, user experience, for personalized and effective healthcare delivery. The global active wearable medical device market reached a valuation of USD 27 billion in 2022, indicative of the growing demand and widespread adoption of these new healthcare solutions. Simultaneously, the active implantable medical device market achieved a value of USD 22 billion, underscoring the significant role of these devices in modern healthcare. The combined size of these two markets is projected to reach USD 100 billion in 2030.^[11]

However, a significant issue affecting the widespread deployment of WIMDs lies in the power sources essential for energizing sensors and actuators, enabling data acquisition, on-board artificial intelligence processing, edge computing, and information communication. Current WIMDs use primary batteries to ensure uninterrupted power supply for their sustained and

Z. Gao, Y. Zhou, J. Zhang, J. Foroughi, S. Peng, C. H. Wang
 School of Mechanical and Manufacturing Engineering
 University of New South Wales
 Sydney, NSW 2052, Australia
 E-mail: chun.h.wang@unsw.edu.au

R. H. Baughman
 Alan G. MacDiarmid NanoTech Institute
 The University of Texas at Dallas
 Richardson, TX 75080, USA

Z. L. Wang
 Beijing Institute of Nanoenergy and Nanosystems
 Chinese Academy of Sciences
 Beijing 101400, P. R. China

 The ORCID identification number(s) for the author(s) of this article can be found under <https://doi.org/10.1002/adma.202404492>

© 2024 The Author(s). Advanced Materials published by Wiley-VCH GmbH. This is an open access article under the terms of the [Creative Commons Attribution](https://creativecommons.org/licenses/by/4.0/) License, which permits use, distribution and reproduction in any medium, provided the original work is properly cited.

DOI: 10.1002/adma.202404492

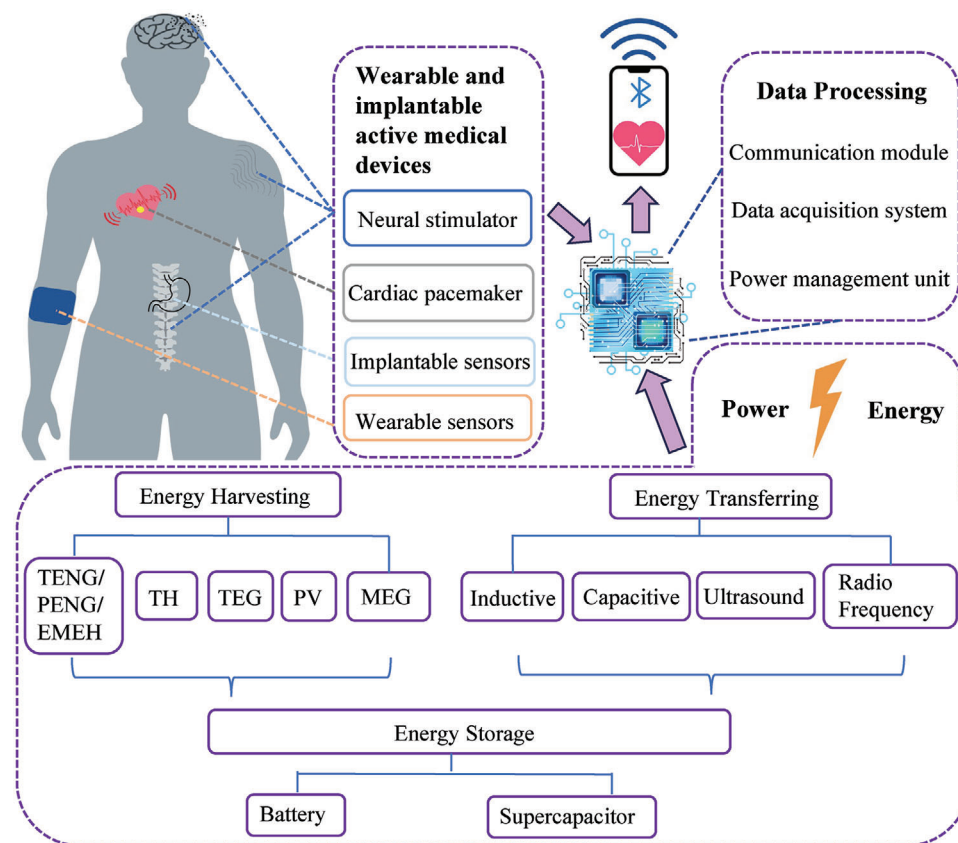


Figure 1. Illustration chart for a future vision where wearable and implanted medical devices, such as neural stimulators, cardiac pacemakers, and sensors, are self-powered, eliminating the need for battery replacements. The power and energy system integrates energy harvesters, wireless energy transfer devices, and energy storage to supply power to the WIMDs. In addition, the system is equipped with modules for power management, data acquisition, and communication. The relationships among energy harvesting devices, energy transfer devices, and energy storage devices are also shown. Abbreviations for various energy harvesting devices include triboelectric nanogenerator (TENG), piezoelectric nanogenerator (PENG), twistrion harvester (TH), electromagnetic generator (EMEH), thermoelectric generator (TEG), moisture-driven energy generator (MEG), and photovoltaic energy harvester (PV).

effective operation, particularly for critical applications. **Figure 1** illustrates a future vision where WIMDs are self-powered, eliminating the need for battery replacements. Energy harvesters, wireless energy transfer devices, and energy storage are integrated to supply power to a diverse range of WIMDs, such as neural stimulators, cardiac pacemakers, and sensors. Wearable and implantable sensors can collect, process, and transmit patient data wirelessly to mobile phones or cloud servers. This feature allows healthcare providers and users to easily access and real-time monitor the patient's health status, enabling timely decision making and improving overall patient management. By eliminating the need for battery replacement or conventional recharging, this system improves patient outcomes. Among implantable devices like cochlear implants, pacemakers, neural stimulators, neuralinks, and retinal implants, power consumptions vary depending on their applications, typically ranging from microwatts to a few milliwatts.^[12] The power consumption significantly affects device miniaturization, determining their physical sizes and durability.^[12] The reliability of WIMDs is also intricately linked with their ability to maintain a steady power supply and vital for functions such as fall detection and cardiac monitoring to predict heart failure. Presently, WIMDs heavily rely on primary or

rechargeable batteries, often with limited lifespans, necessitating periodic replacement, recharging, or surgeries for battery replacement upon depletion. These medical procedures pose infection risks to patients undergoing surgery. Additionally, the size of the battery impacts the overall dimensions of WIMDs, constraining device design and limiting potential implantation sites within the human body.

One promising strategy for overcoming the limited lifespan of primary batteries is to harvest energy from the human body and the surrounding environment. In situations where the energy harvested from the body is insufficient, wireless power transfer technologies can offer a complementary means for charging energy storage devices. For example, induction, capacitive coupling, radio frequency, and ultrasound-induced energy harvesting can charge energy storage devices or power WIMDs directly. The harvested or transferred energy can be used to power WIMDs or to charge energy storage devices. In this way, it is possible to eliminate the use of primary batteries, thus minimizing the risks associated with surgical replacements, enhancing patient experiences and outcomes, increasing the versatility of WIMDs, and lowering the cost by reducing the need for manual charging and maintenance.

Our body is a rich source of energy, generated through fundamental processes like heartbeat, respiration, joint rotations, and body movements. To harness this inherent energy, a range of wearable and implantable energy harvesters have been developed, including mechanical energy harvesters, such as triboelectric nanogenerators (TEGs),^[13] piezoelectric nanogenerators (PENGs),^[14,15] twistrion harvesters,^[16] and electromagnetic generators. They are designed to capture energy from mechanical motions, externally (in vitro) and internally (in vivo). Biochemical energy harvesting technologies, such as glucose fuel cells, can also be used to produce energy within the body through biochemical reactions. Additionally, thermoelectric generators can convert body heat into electricity, while electrochemical energy harvesters, such as moisture electric generators, can extract energy from the humidity gradient in the environment. While these innovative technologies have shown remarkable progress over the past decade, their clinical applications in powering WIMDs remain exceedingly limited.

Beyond the energy produced by our body, there is abundant energy in our surroundings, such as solar energy and electromagnetic fields emitted by Wi-Fi and similar devices. This environmental energy can be captured by wearable energy harvesters or transmitted into our bodies via electromagnetic induction. The harvested or inducted energy can supplement primary or recharging rechargeable batteries, leading to reductions in battery size or even their complete replacement. Therefore, energy harvesting and induction technologies have the potential to transform wearable and implantable medical devices, ushering in a new era of autonomy in personalized medical care. By harnessing these technologies, we can significantly enhance the functionality and performance of WIMDs while also extending their operational longevity.

This review provides a systematic analysis of current and emerging techniques for powering wearable and implantable medical devices, with a primary focus on recent advancements in closing the gap between WIMDs' energy needs and the energy that can be harvested from human bodies or the environment. Beginning with an overview of the typical power requirements of a range of common WIMDs and sensors, this review then assesses the latest advancements in new material technologies aimed at harvesting more energy per unit area or mass, increasing energy storage density, and enhancing wireless power transfer efficiency. Fundamental to these new technologies are advanced materials, especially flexible, stretchable, and biocompatible materials that can be integrated into clothes, worn on the skin, and implanted in our bodies. Some of the most important impacts include increased energy harvesting efficiencies, greater wireless power transfer range, and higher energy or power densities of energy storage devices. Some major types of active medical devices, energy harvesting devices, energy transfer devices, and energy storage devices are illustrated in **Figure 2**. By analyzing their operational principles, performance metrics, limitations, and major case studies, this review offers comprehensive insights into the effectiveness of these approaches. For example, innovations in the design of materials, microstructures, and interfaces have yielded significant enhancements in energy harvesting efficiency, the energy densities of wearable batteries and supercapacitors, and wireless charging efficiency. Finally, the review outlines existing challenges and identifies research oppor-

tunities for accelerating the clinical applications and enhancing the commercial viability of self-powered WIMDs.

2. Power Demands of WIMDs

The power requirements of WIMDs vary significantly, ranging from microwatts (μW) to milliwatts (mW), a spectrum largely dictated by the specific demands of their applications.^[12] Below we provide a comprehensive review of the typical power budgets for a wide range of medical devices, serving as a fundamental reference point for designing and selecting power sources. The typical power demands of ten distinct types of WIMDs are summarized in **Figure 3**, with more detailed analyses of these devices provided in the following sections. It is worth noting that effective powering strategies need to be combined with reduced power consumption to extend the operational lifespan of WIMDs.

2.1. Implantable Medical Devices

2.1.1. Cardiac Pacemakers

The first implantable pacemaker invented by Rune Elmqvist was powered by two nickel–cadmium rechargeable batteries, which had a radio loop antenna attached, enabling the batteries to be recharged each week by beaming radio energy through the skin to the pacemaker's antenna. The initial rechargeable battery had limited recharging lifespan. Coupled with issues of toxicity, the first patient has undergone almost 30 pacemaker replacement surgeries.^[29] Nuclear batteries were investigated for powering pacemakers, boasting a lifespan extension up to 30 years. However, nuclear-powered pacemakers pose travel inconveniences for patients and challenges in the safe disposal of used cells, not to mention the extreme toxicity, hindering their commercial viability.^[30] Lithium-iodine batteries were introduced in 1973 for implantable pacemakers,^[31] offering improved longevity, low current drain, and suitable voltage characteristics. Consequently, lithium and more recently lithium-ion batteries have become the preferred power sources for implantable devices, featuring lifespans exceeding 10 years, reduced manufacturing costs, and compact size. Cardiac pacemakers operate at minimal energy levels, typically $\approx 15 \mu\text{J}$, translating into an annual power usage between 10 and 100 μW . This equates to a battery consumption of 0.5 to 2 Ah over a span of 5 to 10 years, suggesting that a battery with a capacity of 1 Ah could sustain a pacemaker for up to 10 years.^[17] As a result, repeated battery replacement surgeries are needed, which poses significant risks to patients, potentially leading to severe side effects. To address these issues, alternatives to surgeries have attracted significant interest, such as body energy harvesting, which will be discussed in Section 3.

2.1.2. Neural Stimulators

Neural stimulators are active implantable medical devices designed to deliver controlled electrical pulses to nerves or areas of the brain to relieve pain and treat neurological disorders, such as major depressive disorder.^[32] Examples of neural stimulations, which are class III medical devices, include deep brain

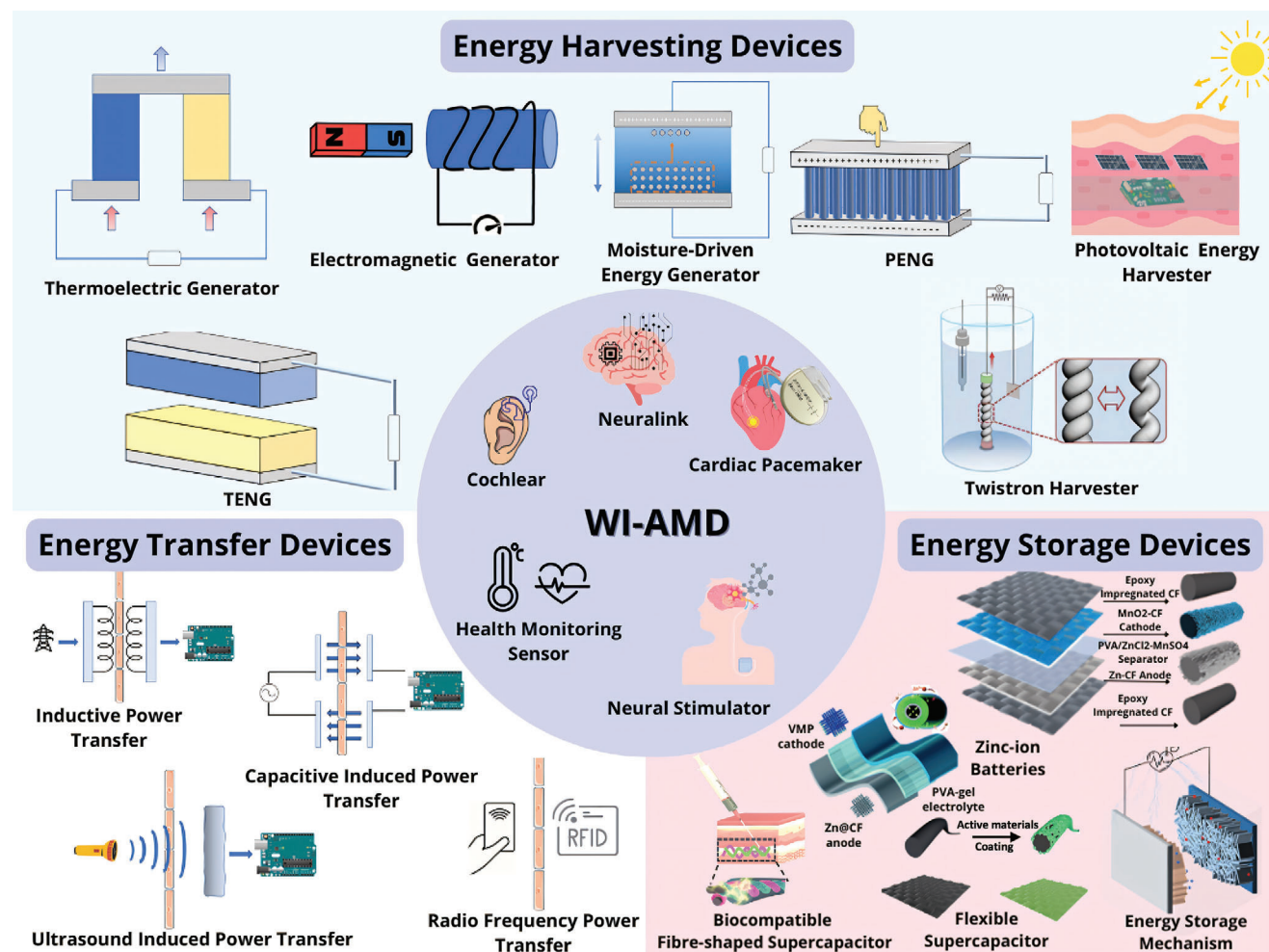


Figure 2. Power harvesting and transfer solutions for WIMDs. The sketch of twistron harvester. Adapted with permission.^[16] Copyright 2017, The American Association for the Advancement of Science.

stimulators, spinal cord stimulators, and vagus nerve stimulators. They were also used to restore lost sensory functions, such as olfaction.^[33] However, neural stimulators generally demand more power than devices used for cardiac pacemakers, presenting a major challenge in developing comparably small-sized devices. The power requirements for neural stimulation devices depend on specific applications.

One important application of neural stimulators is for spinal cord and peripheral nerve stimulation to manage various chronic injuries and pain conditions. Patients received spinal cord stimulation often report a higher quality of life, more noteworthy pain relief, and a return to normal activities and work, compared to those receiving only pharmacological treatments.^[34] As reported by Moore and McCrory,^[18] spinal cord stimulation that operates between 60 and 100 Hz with voltage ranging from 2 to 8 V and pulse width between 100 and 500 μ s, requires power consumption between 24 μ W to 3.2 mW.^[18]

Brain neuromodulation has also shown promise in improving symptoms related to movement disorders.^[35] Deep-brain stimulation, typically operating at voltages of 2 to 10 V,

frequency between 130 and 185 Hz, and pulse widths of 60 to 450 milliseconds, requires an estimated power of 31.2 μ W to 8.325 mW.^[19] Therefore, neuromodulation applications require microwatt-level power, thus demanding larger batteries than those used in pacemakers to sustain consistent functionality.

The power requirements for neural stimulation applications, which demand microwatt-level power for advanced controls, such as varying amplitude, frequency, and pulse width, present a significant challenge to current energy harvesting technologies due to their relatively low output power. It is worth noting that recent research in neural stimulators has explored the direct use of harvested energy for nerve stimulation, bypassing the need for a power supply and power management unit. However, this area of research is still in its initial stages. There is a lack of ability to control the amplitude, frequency, and pulse shape of the signal, and no clinical applications have been reported. This further highlights the existing gap between the power demands of neural stimulation technologies and the potential of energy harvesting solutions. Further discussion will be presented in Section 3.

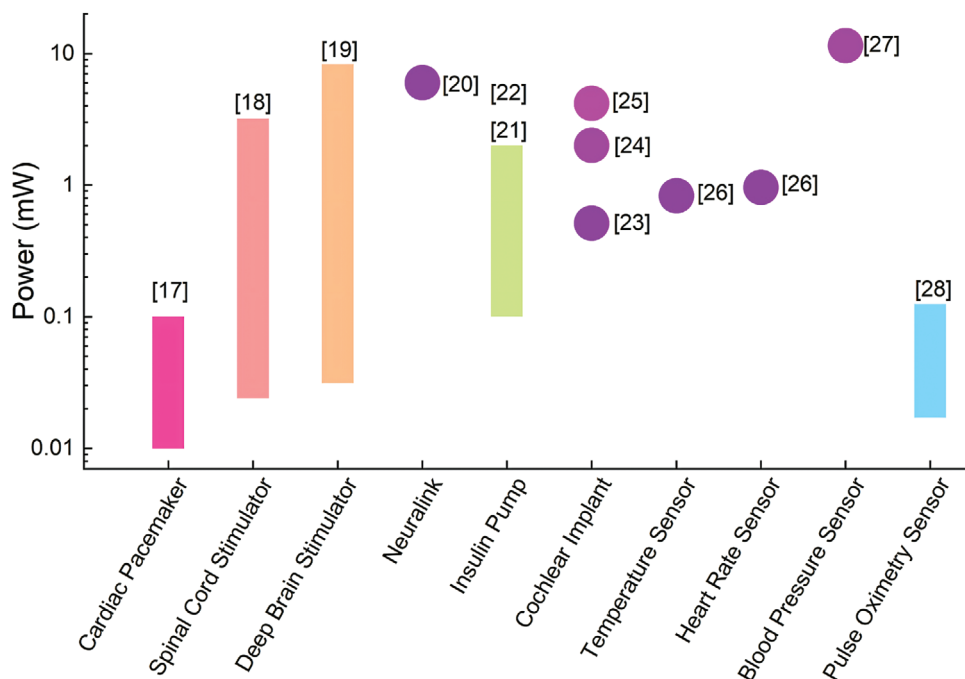


Figure 3. Power demands of ten different wearable and implantable medical devices. These devices are cardiac pacemaker,^[17] spinal cord stimulator,^[18] deep brain stimulator,^[19] neuralink,^[20] insulin pump,^[21,22] cochlear implant,^[23–25] temperature sensor,^[26] heart rate sensor,^[26] blood pressure sensor,^[27] and pulse oximetry sensor.^[28]

2.1.3. Neural Recording for Brain–Machine Interfaces

Brain–machine interfaces can help individuals with a broad range of medical conditions. For instance, controlling soft robotic hands through human neuroprosthetics has been successfully demonstrated.^[36] Furthermore, speech neuroprosthetics has the potential to re-establish communicative abilities for individuals experiencing paralysis.^[37,38] While millisecond and micrometer scales are considered the benchmark for capturing neuronal action potentials for neural recording, a gap remains in developing a microelectrode technology that can be clinically applied for extensive recordings.^[39] Such an advancement would require a design featuring materials known for their excellent biocompatibility, safety, and long-term durability.

To meet the high-bandwidth demands of a brain–machine interface and leverage the benefits of thin-film technologies, Elon Musk’s Neuralink^[20] team has made significant strides toward a flexible, scalable brain–machine interface that expands channel capacity, surpassing previous efforts by a factor of ten. The system comprises three principal elements: ultrathin polymer probes, a neurosurgical robot, and custom high-density electronics. A total of 96 polymer threads were implanted, each containing 32 electrodes, resulting in a total of 3072 electrodes. They have developed and produced over 20 distinct types of threads and electrodes for their arrays. The designs feature either separate threads for reference electrodes or threads that carry both reference and recording electrodes. The threads vary in width from 5 to 50 μm and include various geometries for recording sites. Each thread is typically 4–6 μm thick, which accommodates up to three insulation layers and two conductor layers. The threads are generally 20 mm long. To handle these fragile, lengthy threads

before insertion, a parylene-C film is applied to keep the threads secured. Due to the small surface areas of the individual gold electrode sites, surface modifications are employed to reduce impedance and enhance the charge-carrying efficiency of the interface. They have utilized two treatments: the electrically conductive polymer poly(3,4-ethylenedioxythiophene)–poly(styrene sulfonate) (PEDOT:PSS) doped with polystyrene sulfonate and iridium oxide. Although PEDOT:PSS offers lower impedance, its long-term stability and biocompatibility are not as well established as those of iridium oxide. These electrodes were connected to a custom-designed Neuralink application-specific integrated circuit (ASIC), featuring 256 individually adjustable amplifiers, built-in analogue-to-digital converters (ADCs), and additional circuitry for digitized output serialization. The integrated ADC operates at a sampling rate of 19.3 kHz with a resolution of 10 bits, while the entire ASIC has a power consumption of roughly 6 mW. Neuralink has also engineered compact electronics device capable of simultaneously transmitting electrophysiological data from all the electrodes. This system is encapsulated in a package designed for long-term implantation and is accompanied by custom online spike-detection software, capable of identifying action potentials with minimal delay. Collectively, this cutting-edge research marks the initial step toward achieving a fully implantable brain–machine interface for human use.^[20]

2.1.4. Insulin Pumps

Continuous subcutaneous insulin infusion, more widely recognized as insulin pump therapy, exemplifies the cutting-edge integration of technology into medical care, particularly for

managing type 1 diabetes mellitus. This therapy system comprises an insulin reservoir, an infusion set with tubing and a cannula, a highly efficient pumping mechanism, a computer chip, an interactive screen, a durable casing, and an energy-efficient battery. The growing prevalence of type 1 diabetes on a global scale has propelled the adoption of insulin pump therapy, which utilizes rapid-acting insulin analogs for subcutaneous delivery. This method meticulously replicates the natural insulin secretion of the human body, ensuring that insulin delivery is both consistent and precise which is a crucial aspect for the efficiency and safety of the therapy.

However, the reliability of insulin pumps' power sources remains a critical issue. Failure of the pump's battery or power unit can result in serious, potentially life-threatening, consequences for users. The survey conducted by Murata et al. on 1499 devices revealed that 66 experienced troubles related to their power components, underscoring the urgent need for robust and reliable power solutions.^[40] The power consumptions of these pumps range from 100 μ W to 2 mW,^[21,22] highlighting the diverse power requirements that depend on the device's specific functions and operational settings. In quest of alternative uninterrupted power supply to replace batteries, energy harvesting, and wireless power transfer technologies have recently received significant interest. These innovative approaches, which will be discussed in Section 3, have the potential to enhance the reliability and safety of insulin pump therapy as well as improve the overall user experience by minimizing or eliminating the need for frequent battery replacements or recharging.

2.1.5. Cochlear Implant

A cochlear implant (CI) is an electronic medical device designed to restore the perception of sound for individuals with severe to profound hearing loss by directly stimulating the auditory nerve within the inner ear. This sophisticated device comprises both external and internal elements equipped with a microphone, speech processor, transmitter, and rechargeable or disposable batteries for power.^[41] The type and capacity of these batteries significantly affect how long the implant can function before requiring either a recharge or battery replacement. Yiğit et al. detailed a cochlear implant system that demonstrates an overall energy consumption of 513 μ W.^[23] Meanwhile, Wang et al. introduced a design for cochlear implants characterized by low power consumption, with a total energy requirement of \approx 2 mW when operating at a clock frequency of 3 MHz.^[24] Additionally, Accoto et al. have reported that the electrical energy necessary for stimulating the auditory nerve during typical conversation amounts to 4.17 mW.^[25] Recently, energy harvesting techniques have demonstrated significant potential in supplying power to cochlear implants reliably and continuously, prolonging the operational life of the cochlear implants and enhancing user experience by reducing or completely obviating the need for regular battery changes or recharges.^[42]

2.2. Wearable Health Sensors

Wearable health sensors have significantly evolved to incorporate an array of sensors for comprehensive health monitoring and

telemedicine applications. These sensors can measure body temperature, heart rate, blood pressure, and oxygen saturation levels through pulse oximetry. Dieffenderfer et al. introduced a low-power wearable sensor system designed to link environmental exposure to physiological responses and potential health issues, with a focus on understanding how ozone and other pollutants can exacerbate chronic asthma. The team highlighted the limitations of commercial components for continuous monitoring and outlined their strategies for enhancing device wearability and reducing power needs. Their design included a wristband equipped with a temperature sensor and a chest patch for heart rate monitoring via photoplethysmography. The system reports a power consumption of 0.83 mW for the wristband's temperature sensor and 0.96 mW for the chest patch's heart rate sensors.^[26]

Salo et al.^[27] developed a wearable blood pressure sensor leveraging a monolithically integrated chip based on the topometric principle, allowing continuous blood pressure measurements without invasive methods. This chip, produced using industrial complementary metal-oxide-semiconductor (CMOS) technology and micromachining, is aimed for portability and low energy consumption, requiring only 11.5 mW power to achieve high-resolution blood pressure monitoring and capture detailed waveform features.

Furthermore, portable pulse oximeters, crucial for monitoring essential health indicators, use batteries and consume \approx 90 mW.^[43] The high-power consumption inhibits their applications for continuous daily monitoring. Leveraging organic technology, a new type of reflective patch-type pulse oximetry sensor has been developed with significantly reduced power needs, ranging from 17 to 125 μ W.^[28] The innovation in organic light-emitting diodes and photodiodes, designed through optical simulation to optimize light propagation through the skin, marks a significant step forward in enabling all-day wearable health monitors.^[28]

Self-powered wearable sensors have also witnessed significant growth over recent years,^[44] evolving into active sensors that can convert kinetic, chemical, and thermal energies into electrical energy for real-time human body monitoring. These sensors, designed to conform to the skin's surface, monitor physiological markers by sensing physical movements^[45] and analyzing biofluids.^[3] The electric energy outputs from these self-powered sensors can reduce the power consumption of the power management units discussed in the following section. The essence of this technology lies in leveraging the electrical signals generated as a fundamental detection mechanism. This approach has been extensively adopted for precise measurements of multiple health indicators, including but not limited to joint rotation or skin stretch, temperature, and humidity, making these wearable self-powered biosensors exceptionally efficient in identifying numerous physiological indicators. Self-powered wearable sensors can also potentially serve as energy harvesting devices.^[46] This will also be further discussed in Section 3.

2.3. Power Management Unit

Power management units play a critical role in the functioning of WIMDs, such as regulating how the power from the limited on-board energy source is used for data capture, storage,

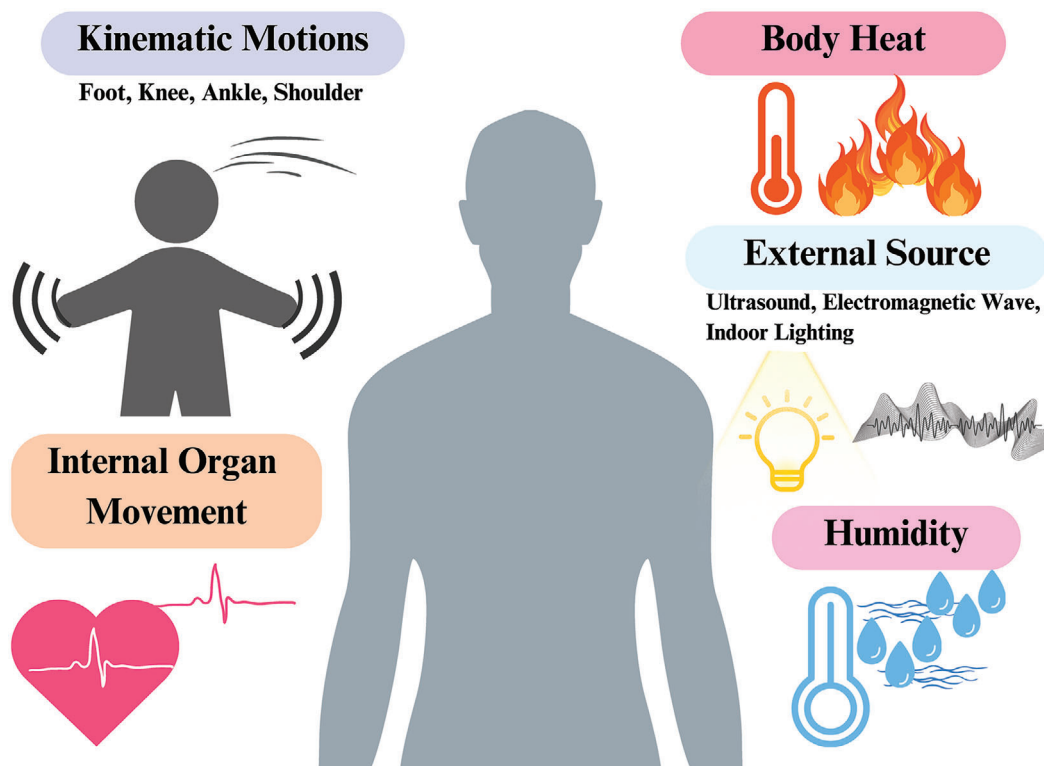


Figure 4. Energy sources available in and around the human body.

processing, and communication. Figure 1 elucidates the framework for achieving an automatic system for health monitoring applications. This system comprises sensors, which can be categorized as either passive or active, an amplifier chip that amplifies the signal, an analog to digital converter that digitizes the sensor output, and a Bluetooth module facilitating wireless transmission of data.^[47,48] The power management system encompasses the entire power circuitry, converting the input voltage from an energy source into different voltage levels tailored for each device element. This system can be charged by wearable and implantable energy harvesters.

To reduce power waste by the power management unit, modern microprocessors scaling through a system-on-a-chip (SoC) approach incorporate a diverse array of components. This includes adaptive circuits, integrated sensors, and advanced power-management techniques with multicore and multifunctional capabilities for integration with energy harvesting technologies, enabling fully autonomous medical operations. The power consumption for SoCs has been minimized to a few microwatts, suggesting that such systems could feasibly be powered by energy harvesting devices to achieve autonomous functionality.^[49,50]

3. Energy Harvesting Technologies for Powering WIMDs

Energy harvesting technologies capable of harnessing energy from the human body, or the surrounding environment hold tremendous promise for replacing primary batteries upon which WIMDs currently depend. These technologies offer several key advantages, including reducing the risk of infection associated

with battery replacement in implanted medical devices, enabling miniaturization by reducing the size of batteries needed to store harvested energy, and enhancing user comfort and convenience by eliminating the need for periodical battery replacement or recharge. Figure 4 illustrates distinct locations around the human body and organ systems within the body that can be tapped into to harvest energy, including organ and body motions, thermal energy, humidity, as well as external sources like ultrasound, electromagnetic waves, and light.^[51] Mechanical energy sources typically manifest at lower frequencies, ranging from 0 to 20 Hz.^[52] One significant benefit of harvesting mechanical energy from inherent physiological movements, such as the rhythmic expansion and contraction of the chest or internal organs, is their continuous occurrence throughout both the day and the night. This consistency ensures a steady and uninterrupted energy output. While a substantial portion of this energy is naturally utilized to support the body's regular functions, a significant amount of energy remains untapped and dissipates into the surroundings. These untapped energy reserves present a valuable opportunity. When effectively captured and converted, they have the potential to generate electrical energy capable of powering implantable medical devices. This paves the way for establishing a more sustainable and efficient power solution for essential healthcare applications.

In the following sections we will examine recent advances in flexible, stretchable, and high-performance energy harvesters to harness mechanical energy from the human body and electromagnetic energy in the surroundings. For example, nanogenerators such as TENGs,^[13] PENGs,^[15] and electromagnetic generators^[53] can be used to harness energy from human body motion.

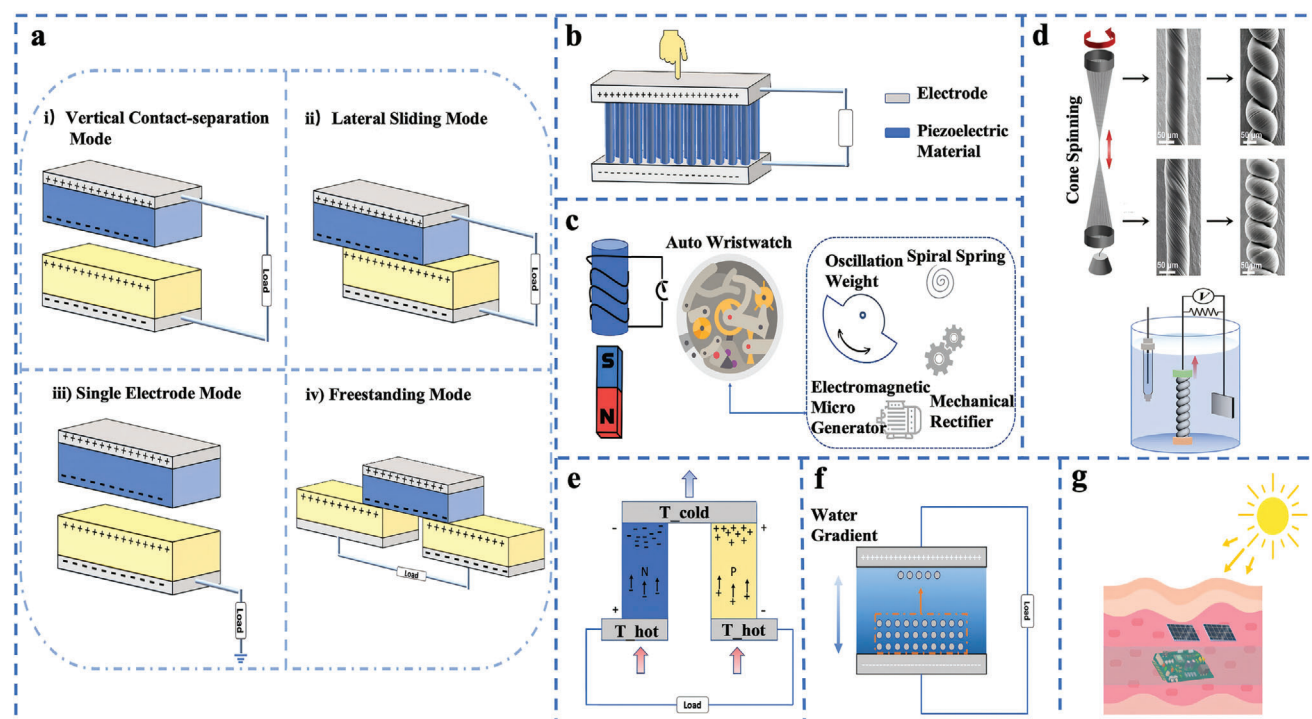


Figure 5. Working principles of six types of energy harvesting technologies. a) TENG. b) PENG. c) Electromagnetic generator. d) Twistron harvester. Adapted with permission.^[16] Copyright 2017, The American Association for the Advancement of Science. e) Thermo-electric generator. f) Moisture-driven energy generator. g) Photovoltaic device inside the human body to harvest energy from solar and indoor lighting.

3.1. Harvesting Energy from the Human Body

Although significant mechanical energy can be produced through everyday human movements/motions like those involving the arms, fingers, chest, knee, ankle, and heel, harnessing this energy effectively presents a significant challenge.^[54] Among the many energy harvesting techniques reported in the recent literature, seven types have demonstrated the most versatility and high-energy harvesting efficiencies, including triboelectric, piezoelectric, electromagnetic, photovoltaic, thermal, and mechanical–electrical–chemical methods, which will be reviewed below.

3.1.1. TENGs

TENG was first demonstrated by Wang's group in 2012 by employing Kapton and polyester as the triboelectric layers to harness energy from mechanical deformation.^[55] Integrating the effects of triboelectrification and electrostatic induction, TENGs can convert mechanical energy into electricity. Compared to PENGs, TENGs can produce significantly higher voltage and power, making it possible to directly charge capacitors or supercapacitors. With the ease of fabrication and cost-effectiveness, TENGs provide a promising approach to harvesting energy from mechanical movements. In addition, TENGs can serve as self-powered sensors that would reduce the system's power consumption.

A typical TENG consists of an electrode and a dielectric material. Upon exposure to an external mechanical force, triboelec-

tric charges develop on the two contact surfaces. The charge density builds up under repeated pressure loads and can reach the maximum value after a few cycles. Wang^[56] presented four fundamental working modes of TENG: normal contact–separation, lateral sliding, single electrode, and freestanding triboelectric layers, as illustrated in **Figure 5a**. Among these four modes, the normal contact–separation model has shown the most promise, as the other three modes are not suitable for harnessing mechanical energy from the human body, and hence will not be further discussed in this section.

The normal contact–separation mode is a widely employed TENG operation, which typically comprises two electrets of different electric polarities, two back electrodes, and an external circuit, as shown in **Figure 5a**. When the two electrets come into contact, electrification occurs due to local frictions between the two surfaces, generating opposite charges on the two electrets. The charges then induce an electrostatic field across the two electrodes when the two electrets separate, producing an alternating current in an external circuit. The electrets or the triboelectrical layers serve several vital functions crucial for the TENGs' operation and effectiveness. Made of dielectric materials with very low electrical conductivity and high dielectric constant, the electrets generate charges through contact or friction. The charges are typically stored on the contacting surfaces of the electrets. The greater the surface charge density, the higher the energy output of TENGs. Effective strategies to enhance the energy harvesting efficiency of TENGs include maximizing the surface area and incorporating fillers to increase the dielectric constant of electrets. Common materials used for this purpose include

conductive fillers such as graphene and metal nanoparticles,^[57] dielectric metal oxides or ceramic particles, and hybrid of these materials.^[58] The mechanical properties of electrets are also very important, as they play a pivotal role in TENGs' durability and stability.

The primary function of the electrode is to facilitate the transfer of electrical charge.^[59] One of the significant obstacles in creating fully wearable TENG devices is the development of a suitable electrode. Conventional metals such as copper and aluminum are widely used for traditional electrodes due to their excellent electrical conductivity. However, the primary challenge with these materials in wearable electronics is their rigidity, which impedes the flexibility and stretchability required for wearable devices. This high stiffness can significantly affect the wearability and functionality of the device by limiting its ability to deform and conform to various movements and shapes of the human body.

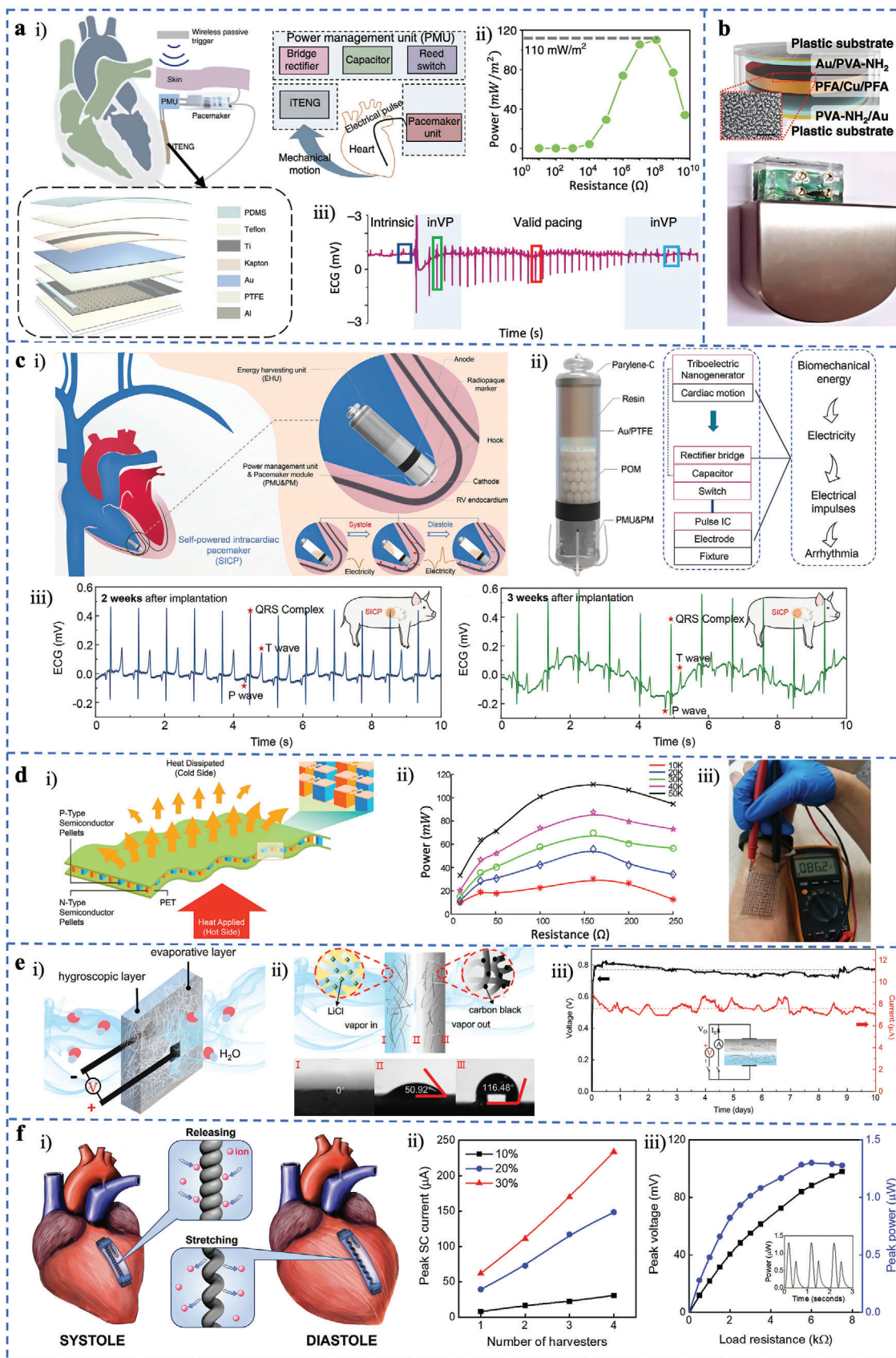
To address this issue, various fabrication strategies have been employed. These strategies include designing suitable geometries and integrating materials that combine flexibility with electrical conductivity while maintaining necessary rigidity.^[60–64] This balance of mechanical and electrical properties is crucial for developing high-performance, fully stretchable electrodes that can maintain their functionality under the mechanical strains experienced in wearable and implantable applications.

The energy produced by a TENG can be stored in an energy storage device, such as a capacitor, via a rectifier to convert the alternating current (AC) output to direct current (DC). Due to the high voltage outputs of TENGs, charging can be achieved without needing powered amplifiers. This method can be readily integrated into clothing to capture energy from everyday activities like chest expansion, walking, and arm movements. Additionally, it can capture energy from movements within the internal organs, such as pressing, bending, and the heartbeat.^[65] TENGs can harvest energy under small sliding or opening displacements. However, appropriate encapsulation of the device is essential to mitigate the negative impact of the aqueous human body environment on the triboelectric performance.

TENGs have demonstrated significant potential in powering WIMDs through two major modes: 1) harvesting energy and storing electricity in a battery or capacitor, and 2) utilizing their electrical outputs to directly energize WIMDs. In 2019, Ouyang et al. introduced a pioneering symbiotic cardiac pacemaker that could harvest and store energy and maintain stable cardiac pacing in animal models.^[65] The device utilized a TENG to harvest energy from heart movement which was then stored in a power management unit through a rectifier. An external wireless magnet switch was used to activate the pacemaker, as shown in **Figure 6a(i)**. To enhance the surface charge density and boost the output from the energy harvesting device, a corona discharge technique was applied to the surface of the polytetrafluoroethylene (PTFE) triboelectric layer. The peak power density reached 110 mW m^{-2} at a load resistance of $100 \text{ M}\Omega$ (**Figure 6a(ii)**). The energy harvester demonstrated exceptional durability, functioning effectively even after 100 million mechanical test cycles, achieving a maximum open-circuit voltage of 65.2 V and a short-circuit current of $0.5 \text{ }\mu\text{A}$. The energy harvested from one cardiac cycle was $0.495 \text{ }\mu\text{J}$, sufficient to power the pacemaker. Some common patterns including intrinsic rhythm and valid pacing of ECG had been ob-

served during the pacing process by symbiotic cardiac pacemaker system as illustrated in **Figure 6a(iii)**. Furthermore, Ryu et al.^[66] introduced a high-performance, inertia-driven triboelectric energy harvester based on gravity difference caused by body motion, which can successfully charge a lithium-ion battery inside a pacemaker, as illustrated in **Figure 6b**. These five-stacked TENGs can generate a peak power of up to $4.9 \text{ }\mu\text{W cm}^{-3}$. In 2024, Liu et al.^[67] introduced a self-powered intracardiac pacemaker (SICP) that utilizes nanogenerator technologies to harvest biomechanical energy from cardiac motion in a swine model. The innovative device, featuring a capsule structure, is designed for insertion into the right ventricle via a delivery catheter through an intravenous route (**Figure 6c(i)**). The SICP is comprised of an energy harvesting unit, a power management unit, and a pacemaker module (as shown in **Figure 6c(ii)**). Laboratory experiments revealed that the device produced an open-circuit voltage (V_{oc}) of $\approx 21.8 \text{ V}$, a peak short-circuit current (I_{sc}) of $0.25 \text{ }\mu\text{A}$, and a short-circuit charge (Q_{sc}) of 6.4 nC . Impressively, it achieved a maximum output power density of 2200 mW m^{-3} at an external resistance of $100 \text{ M}\Omega$. The ECG signals of the experimental animals were tracked for two and three weeks, respectively (**Figure 6c(iii)**). During this time, the heart rhythm was stable, and the experimental animals continued to eat and live normally without the occurrence of complications. This pioneering work suggests a viable minimally invasive method for biomechanical energy harvesting, potentially extending the service life of leadless pacemakers significantly.^[67]

TENGs are also widely used for developing self-powered neural stimulators. Jin et al. introduced a self-powered functionalized implantable neural electrode system (FI-NES) aimed at nerve restoration, by integrating a novel tribo/piezoelectric hybrid nanogenerator based on a multifunctional nanoporous nerve guide conduit (NP-NGC). A conductive nerve guide conduit (NGC) must meet specific criteria for long-term repair of peripheral nerve injury, such as biocompatibility, porosity, and mechanical strength, while also requiring appropriate electrical conductivity ($>10^{-1} \text{ S cm}^{-1}$). A structural design strategy was introduced to create a multilayer NP-NGC. In this design, naturally biodegradable chitosan (CS) was electrospun into nanofibers to form the inner layer. Then, PEDOT:PSS is coated onto the surface of these CS nanofibers. The PEDOT:PSS was subsequently treated with an optimized H_2SO_4 process to induce recrystallization of the PEDOT molecular chain. This process resulted in CS/PEDOT nanofibers with a core/shell structure, where the conductive PEDOT layer around a thickness of 30 nm tightly envelops the CS nanofibers. This conduit exhibited superior mechanical properties, porosity, conductivity, and degradability. The hybrid nanogenerator, characterized for its electrical performance using an auto step motor, achieved an open-circuit voltage of $501 \pm 8 \text{ V}$ over a 16 cm^2 working area, with the frequency of the pressure having no impact on its electrical performance. It reached a maximum power density of 72 mW m^{-2} , sufficient to illuminate 15 light-emitting diodes (LEDs) and charge a $1 \text{ }\mu\text{F}$ capacitor to 5.6 V in 400 s . Postimplantation, the devices, $\approx 1 \text{ cm}^2$ in size, produced peak-to-peak voltage (V_{pp}) and peak-to-peak current (I_{pp}) of 2.7 V and $0.12 \text{ }\mu\text{A}$ in active states, and 2.2 V and $0.1 \text{ }\mu\text{A}$ in calm states, respectively. By the 12th week, the FI-NES system generated $1.5 \pm 0.11 \text{ V}$, still significantly above the 100 mV needed for effective nerve electrical stimulation. After three



months of animal clinical trials, this fully implantable neural electrical stimulation system proved highly efficient in peripheral nerve restoration, equating to the effectiveness of the clinical gold standard, nerve autograft.^[68]

TENGs have also been explored as self-powered sensors to reduce the energy needs of the sensor system for health monitoring. Li et al. proposed a self-powered temperature monitoring platform designed for the continuous and real-time observation of skin temperature in pregnant women and the surrounding environmental temperature.^[69] By coupling a TENG device containing 30 μm PVDF film and a thin Cu foil served as the negative and positive triboelectric layer with a single yarn-based temperature sensor in series, an output voltage was found to be proportional to temperature change. The platform reached the maximum output voltage of 50.1 V, a short-circuit current of 23 μA , and a peak power density of 0.24 W m^{-2} at a load resistance of $\approx 30 \text{ M}\Omega$. Additionally, the sensor's data were transmitted to a mobile phone via Bluetooth module for real-time tracking of skin and ambient temperatures during physical activities. The results suggested a viable route toward the development of self-powered temperature sensing platforms with wide-ranging applications.^[69] On another front, He et al. developed a multiarch strain sensor utilizing PEDOT:PSS-functionalized textile, boasting a vast sensing range. This sensor capitalized on the optimized triboelectric properties of the textile and its energy harvesting capabilities. Remarkably, it generated a maximum output power of 3.26 mW from foot stepping at a frequency of 2 Hz on a $4 \times 4 \text{ cm}^2$ layer of PEDOT:PSS-coated textile. This corresponds to a power density of 2 W m^{-2} harvested from human walking at 2 Hz, with the TENGs' matching impedance being as low as 14 $\text{M}\Omega$. Four self-powered sensors based on the smart textiles were developed and affixed to various human body parts to monitor activities like standing, walking, running, arm bending, sudden falls, and sitting, showcasing the versatility and potential of self-powered sensors in activity monitoring.^[70]

To boost the output power of TENGs, significant progress in material designs and manufacturing processes has been reported. For example, electrospinning has been employed to fabricate high-performance triboelectric layers.^[71] He et al. introduced an innovative Schottky junction-based TENG, employing an electrospun nanofiber mat embedded with hybrid metal-perovskite oxide fillers (PVDF-HFP/Mn-BNT-BT/AgNWs) as the

tribo-negative layer. This configuration yielded an impressive maximum open-circuit voltage of 2172 V and a peak power density of 47.3 W m^{-2} , surpassing the performance of conventional PVDF-based TENGs. Remarkably, this advanced hybrid TENG could illuminate 80 LEDs and power a standard seven-segment LED module to display "2022."^[72] In another significant development, Sha et al. explored an innovative method to enhance the electrical output of TENGs based on the PVDF copolymer by incorporating liquid metal Galinstan. This combination resulted in an almost twelvefold increase in the output voltage. Consequently, this enhanced TENG was able to successfully power an array of LEDs and a series of standard seven-segment digit LED modules.^[73] These advancements highlight the potential of material modification strategies in improving the performance and expanding application possibilities of TENGs in energy harvesting and powering electronic devices.

3.1.2. PENG

Piezoelectric energy harvesting devices can convert mechanical energy into electrical energy via the piezoelectric effect as shown in Figure 5b.^[14] A cyclic pressure variation produces an alternating voltage.^[74] The performance of piezoelectric energy harvester highly depends on structural design and materials, which can be categorized into four types, including single crystals, ceramics, polymers, and composites.^[75]

The composition of PENGs strongly influences their outputs but also plays a critical role in determining their biocompatibility, which is highly dependent on the choice of materials used.^[76–82] Single-crystalline lead magnesium niobate-lead titanate (PMN-PT) and lead magnesium niobate-lead zirconate titanate are efficient piezoelectric ceramic materials with some of the highest piezoelectric coefficients.^[83] However, lead-containing piezoelectric crystals and ceramics pose a health risk due to their toxicity. To address this issue, lead-free piezoelectrical materials have been developed as alternatives for biomedical applications. One major candidate for biocompatible PENGs is zinc oxide (ZnO).^[77] As a semiconductor, ZnO can be synthesized into nanowires or thin films that can convert mechanical deformation such as bending or compression to electricity.^[80] This capability allows ZnO-based PENGs to serve both as energy harvesters for

Figure 6. Energy harvesting technologies. a) (i) Symbiotic cardiac pacemaker system with an energy harvester, power management unit, pacemaker, and wireless passive trigger. (ii) Peak power density at different load resistances. (iii) Simultaneously recorded electrocardiography by symbiotic cardiac pacemaker system. Adapted with permission.^[65] Copyright 2019, The Author(s). b) Internal structure of energy harvester and image of self-powered cardiac pacemaker. Adapted with permission.^[66] Copyright 2021, The Author(s). c) (i) Schematic depiction of the device located in the right ventricle (RV) for transforming biomechanical energy from cardiac movement into electricity and regulating arrhythmia. (ii) The internal structure of the device comprised of an energy harvesting unit, a power management unit, and a pacemaker module. (iii) ECG signal from animal model 2 weeks and 3 weeks after implantation of the device. Adapted with permission.^[67] Copyright 2024, The Author(s). d) (i) Illustration chart of thermoelectric nanogenerator. (ii) Power output at different load resistance. (iii) Demonstration of harvesting thermal energy from human skin by thermoelectric nanogenerator. Adapted with permission.^[102] Copyright 2019, American Chemical Society. e) Design and electrical performance characteristics of a moisture energy generator. (i) Layout of the dual-layer device, which includes a moisture-absorbing layer and a layer for evaporation, each with carbon tape electrodes attached to their outer surfaces. (ii) Side view diagram of the device structure. The water contact angles for the moisture-absorbing layer (I), the interior (II), and the exterior (III) of the evaporation layer are displayed above. (iii) Continuous open-circuit voltage (shown in black) and short-circuit current output (shown in red) from the device under normal room conditions ($25 \pm 2 \text{ }^\circ\text{C}$, RH $60 \pm 5\%$) over 10 days. The average values of the open-circuit voltage and the short-circuit current output are indicated by black and red dashed lines, respectively, with the relevant circuit model shown in the diagram. Adapted with permission.^[109] Copyright 2022, The Author(s). f) (i) Illustration of a twistron harvester positioned on the surface of the heart, demonstrating its method for generating electricity from the heartbeats. (ii) Maximum currents at different strain levels versus the number of harvesters connected in parallel. (iii) Peak voltage and peak power relative to load resistance for four devices connected in series and subjected to a 20% sinusoidal strain at a frequency of 1 Hz. Adapted with permission.^[96] Copyright 2024, The Author(s).

powering small electronic devices and as sensitive sensors for various applications, including pressure monitoring.^[84,85] Moreover, ZnO's stability, biocompatibility, and ability to be deposited on flexible substrates enhance its suitability for energy harvesters and self-powered sensors. For instance, Chaudhuri et al. in 2017 employed ZnO as a piezoelectric material to charge the battery of a cochlear implant,^[42] demonstrating the potential of biocompatible piezoelectric materials as an energy source for powering active medical devices.

Another approach to addressing the toxicity of PZTs is to encapsulate them with biocompatible materials, such as PDMS and PTFE.^[86] Novák et al. demonstrated an encapsulation strategy for implanted circuit boards by using a two-part PVDF mold.^[87] An additional biocompatible layer was added using an inert P3HT polymer coating. The biocompatibility of this encapsulated device was tested according to ISO10993, demonstrating superior robustness compared to PDMS encapsulation only. The complete devices was evaluated *in vivo* to verify their long-term stability.^[88]

For practical applications of providing power to cardiac pacemakers by PENG, Azimi et al.^[89] in 2021 reported a piezoelectric energy harvester capable of a maximum energy output 0.487 μJ per heartbeat. The maximum open-circuit voltage was 4.55 V and the short-circuit current was 2.95 μA with a maximum power density of 140.82 $\mu\text{W cm}^{-3}$. However, the performance of these energy harvesters is yet to be tested and validated in real-world clinical conditions, although some devices have been tested in open-chest conditions while significant reductions in energy output have been found when implanted in a closed chest for long-term operations.^[90]

To address the above-mentioned reduced performance under enclosed chest conditions, Li et al. reported a different cardiac piezoelectric energy harvester to closely mimic real-life conditions.^[91] This device was successfully implanted in a porcine heart for over two months, during which time it demonstrated stable performance and maintained consistent output levels, thereby confirming its exceptional durability. Moreover, the device did not show any infection or significant heart tissue damage. However, a significant drop in the peak-to-peak voltage of this piezoelectric energy harvester was observed in enclosed chest conditions within the initial three days of implantation, dropping from 2 to 0.75 V.^[91]

Transitioning from cardiac pacemakers to health monitoring areas, the team led by Rogers showcased a 3D piezoelectric microsystem that brought new capabilities to the field of sensing and energy generation in 2018.^[92] Their work introduced new avenues for applying these 3D piezoelectric systems across various architectures tailored for harvesting energy, aiding robotic prosthetics, and enhancing biomedical implants. The 3D piezoelectric microsystem incorporates a thin functional layer of PVDF along with two backing electrodes composed of Cr/Au layers. Through experimental study, computational modeling, and theoretical analysis, they illustrated the potential of these systems for capturing energy from multidirectional and broad-spectrum vibrations, converting mechanical forces into electrical energy across a wide range of pressures, sensing mechanical forces in terms of their magnitudes and directions, and harvesting biomechanical energy within the body. Notably, an application was demonstrated through the implantation in a mouse's leg, where no electrical output was observed until the mouse began to move

postanesthesia, producing voltages up to $\approx 100 \mu\text{V}$, and upon full recovery. When the mouse resumed normal activities, the piezoelectric harvester generated a peak voltage above 1 mV. The unique 3D design of these systems facilitates deformation under external forces, ensuring effective energy coupling with muscle movements without causing irritation or significantly hindering natural actions. The 3D piezoelectric microsystems' high energy harvesting efficiency and output voltage demonstrated their potential as implantable devices for both energy generation and sensing purposes.^[92]

Furthermore, Park et al. presented a self-powered flexible piezoelectric pulse sensor leveraging a PZT thin film as piezoelectric thin film and gold as electrodes, tailored for a real-time healthcare monitoring system.^[93] This innovative piezoelectric pulse sensor was incorporated into a signal processing circuit that included amplifiers, comparators, and output modules. The integration enabled the sensor to accurately detect the minute arterial pulse, as depicted. The captured pulse signal was then wirelessly communicated to a smartphone, facilitating a real-time monitoring system using a microcontroller and a Bluetooth transmitter.^[93]

3.1.3. Twistron Harvester

Electrochemical mechanical energy harvesters exploiting stretch-induced changes in capacitance have demonstrated impressive performance. Baughman and colleagues^[16] reported a twistron harvester comprising a twisted and coiled carbon nanotube yarn and a high-surface-area sulfur-rich counter electrode immersed in an aqueous electrolyte. Given the chemical potential difference between a carbon nanotube yarn and an electrolyte, which varies based on the electrolyte's acidic or basic nature, immersing the carbon nanotube (CNT) yarn in an electrolyte can induce an equilibrium charge on the yarn (Figure 5d).^[16] When the CNT yarn electrode is stretched, it increases density and reduces electrochemical capacitance, which in turn causes the voltage to increase to enable energy harvesting.

Utilizing coiled carbon nanotube yarns, the twistrons exploit stretch-induced changes in electrochemical capacitance to convert mechanical energy into electricity. The elongation of the twisted and coiled carbon nanotube yarn causes the transfer of coiling twist to yarn twist, which produces yarn densification and a resulting decrease in yarn capacitance that enables mechanical energy harvesting as electricity. Without the need for an external power source to maintain bias voltage, stretching coiled yarns generated 250 W kg^{-1} of peak electrical power when cycled up to 30 Hz, as well as up to 41.2 J kg^{-1} of electrical energy per mechanical cycle, when normalized to harvester yarn weight.^[16] For example, at 1 Hz and 5% peak strain, the twistron can generate 350 W kg^{-1} , which is equivalent to 12 mW cm^{-2} .^[94]

They introduced plied twistrons as an alternative to coiled ones, boosting the energy conversion efficiency of the yarns from 7.6% to 17.4% for stretching and up to 22.4% for twisting.^[94] This enhancement is attributed to additional harvesting mechanisms involving yarn stretch and lateral deformations. For mechanical energy harvesting within the frequency range of 2 to 120 Hz, plied twistrons exhibit higher gravimetric peak power and average power compared to nontwistron, material-based

harvesters. The twistrans were integrated into textiles for sensing and harvesting human motion, deployed in saltwater environments for harvesting ocean wave energy, and utilized for charging supercapacitors.^[94] Twistran harvester is a promising candidate for application in implantable devices due to its compact size, stability, and mechanical durability.^[95] However, the high-level applied strain, typically 20%, needed to achieve the power output may limit their applications to specific situations where no such large strain is available.

Recently, Ruhparwar et al.^[96] demonstrated a novel twistran harvester, comprising coiled carbon nanotube yarn, which converts the mechanical energy of the beating heart into electricity. In preparation for implantation in a porcine heart, they characterized the performance of the twistran when artificially stretched at different frequencies, mimicking the deformation pattern of the cardiac surface (Figure 6f(i)). The twistran reached a maximum peak power of 1.42 W kg^{-1} and an average power of 0.39 W kg^{-1} for the 60 beats per minute deformation frequency and the tensile deformation provided by an artificial heartbeat system. Furthermore, for an artificial heartbeat system, when four twistran harvesters were linked in parallel and mounted on the surface of a water-filled rubber balloon that was periodically deformed to 30% sinusoidal strain, they collectively generated a maximum peak short-circuit current of $230 \mu\text{A}$ (Figure 6f(ii)).^[96] As illustrated in Figure 6f(iii), when these four harvesters were connected in series and cycled at 1 Hz and 20% peak strain, they generated $0.338 \mu\text{J}$ of energy per cycle for an external load resistance of 6 k Ω . This energy output is comparable to the threshold energy needed for pacing a human heart ($0.377 \mu\text{J}$), which is higher than the $0.262 \mu\text{J}$ energy required for pacing a porcine heart.^[96] Upon in vivo implantation onto the left ventricular surface of a porcine heart, the device continuously generated electricity from cardiac contraction. The generated energy was utilized for direct pacing of the heart, as confirmed by electrophysiological mapping. The results indicate that twistran harvesters are a promising way to harvest biomechanical energy from cardiac motion to provide the electricity needed for cardiac pacing.

3.1.4. Electromagnetic Generator

Electromagnetic generators (Figure 5c) operate based on Faraday's law of induction. Conventional electromagnetic power generation devices are typically large and heavy, operating at high frequencies. When used to harvest mechanical energy from the human body, these devices can become burdensome. Furthermore, the mechanical energy obtained from everyday human activities tends to have low frequency and small amplitude, resulting in a limited energy output from electromagnetic generators. Despite these challenges, considerable efforts are being made to develop wearable electromagnetic energy harvesters. For instance, Maharjan et al. proposed a high-performance, cycloid-inspired wearable electromagnetic generator capable of delivering an average power of 8.8 mW under excitation vibrations of 5 Hz at a load resistance of 104.7 Ω .^[53]

Moreover, the automatic wristwatch exemplifies a successful electromagnetic generator that can produce useful power by converting human motion into electrical energy.^[97] It harnesses wrist movement as its power source: an eccentric oscillating

weight winds a spring during wrist movement, causing a pinion to rotate. Within milliseconds, a miniature electrical generator, driven by the pinion, generates electrical energy, charging a storage device such as a rechargeable battery. This energy conversion mechanism has been adapted to capture mechanical energy from heartbeats in vivo. Zurbuchen et al. explored a clockwork mechanism adapted from an automatic wristwatch to the motion of heartbeats into electrical energy.^[98] In 2017, they demonstrated the feasibility of battery-free cardiac pacing using a custom-made pacemaker powered by an energy-harvesting mechanism driven by a Swiss wristwatch. The watch could generate an average power ranging from 10 to 90 mW.^[98] They also conducted research to enhance the sensitivity of this mechanism to heart motions by optimizing the oscillator weight, which increased from 7.2 to 16.7 g.^[99]

3.1.5. Thermoelectric Generator

In addition to the mechanical energy derived from human movement, the thermal energy produced by the human body represents another valuable energy source that can be harvested and utilized. Given the relatively consistent body temperature and temperature differential with the external environment, thermoelectric generators offer a stable energy supply. These generators operate based on the Seebeck effect, which involves the diffusion of electrons driven by temperature gradients as seen in Figure 5e.

Considerable research has been devoted to flexible thermoelectric generators employing both inorganic and organic thermoelectric materials. For instance, Kim et al. developed a flexible thermoelectric generator that mimics human skin utilizing body heat to generate power and achieving an output of $\approx 2.28 \mu\text{W cm}^{-2}$.^[100] Similarly, Choi et al. designed an ultralight and flexible thermoelectric generator using carbon nanotube yarn exhibiting remarkable thermoelectric efficiency.^[101] Their device comprised of 60 pairs of n- and p-doped carbon nanotube yarns and reached a peak power density of $10.85 \mu\text{Wg}^{-1}$ with a temperature difference of 5 K.

Moreover, in health monitoring and human activity tracking, body temperature as a vital sign can indicate a range of health states. Body core temperature is tightly controlled within a strict range of 36–37 °C, with any fluctuations outside this range potentially signaling fever, changes in heart rate, and various other health issues.^[2] Feng et al. demonstrated a flexible and wearable thermoelectric nanogenerator characterized by its stable long-term operation at high voltages and output power densities (Figure 6d(i)).^[102] Figure 6d(ii) displays the power output curve of the energy harvester, which varies according to load and temperature difference. The graph illustrated that at a temperature difference of 50 K, it generated a peak power of 113.6 mW and a power density of 11.14 mW cm^{-2} , demonstrating its capability to harvest thermal energy from human skin shown in Figure 6d(iii). It also served as a flexible self-powered temperature sensor with a 0.5 K temperature resolution.^[102]

Despite these promising developments, thermoelectric generators encounter significant challenges. These devices rely on temperature differentials; however, the human body tends to maintain a consistent internal temperature and the internal

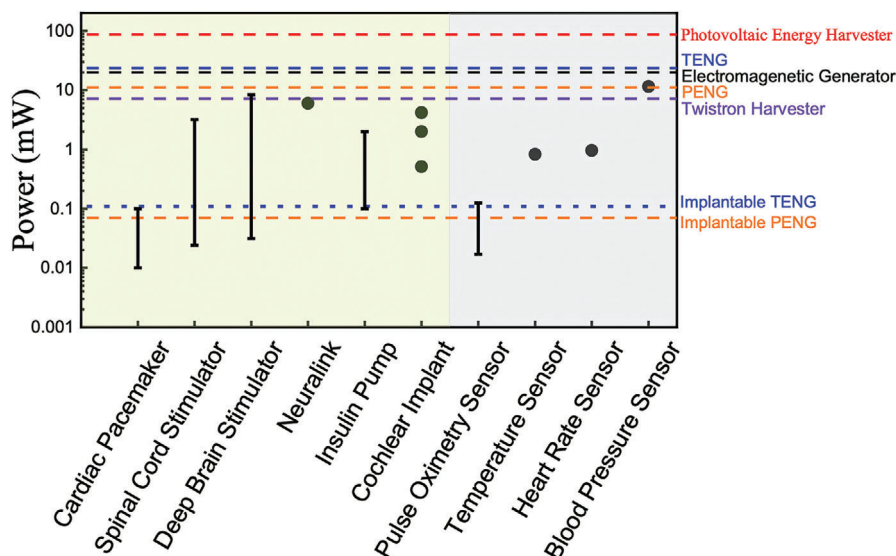


Figure 7. Comparison of the power outputs of energy harvesters around 5 cm^2 with the power needs of a) implantable active medical devices (highlighted in green) and b) wearable sensors (highlighted in gray). Photovoltaic energy harvesters were under 1000 W m^{-2} solar irradiation.^[115,117,118]

temperature variations are often insufficient to generate significant electricity. The typical temperature gradient between the skin and surrounding air, $\approx 10 \text{ K}$, can only produce thermoelectric power in the tens of microwatts per square centimeter range.^[103] Thus, the power density of current thermoelectric generators is inadequate for powering electronic devices as shown in **Figure 7**. Moreover, the utilization of thermoelectric generators in implantable devices presents an even greater challenge, since the internal temperature of the human body remains relatively uniform, without sufficient temperature gradient for these generators to function effectively.

3.2. Harvesting Energy from the Environment

3.2.1. Moisture-Driven Energy Generator

Moisture-driven energy generators (MEGs) stand out for their simplicity and ease of assembly. They also can be readily constructed from a variety of low-cost materials. By designing electrodes to achieve different water diffusion properties, MEGs can utilize water found in natural environments to generate an ion gradient to produce power,^[104] generating electricity from the atmospheric moisture, as illustrated in **Figure 5f**. This process, driven by ion diffusion^[105] and streaming potential,^[106] hinges on the electrochemical dynamics at the water–solid interface and is not limited by geographical or environmental constraints. The mechanism for MEG is attributed to the dynamic electric double layer owing to the transfer of charges at the vicinity of the interface and the change in liquid coverage surface area.^[107] Significant theoretical and experimental work has advanced MEGs, with evaporation generators standing out for their ability to transform thermal energy from the air into sustainable electricity until the water has entirely evaporated.^[108] Similarly, humidity-driven generators depend on the ambient moisture to produce electricity.^[104]

Tan et al. proposed a novel device that can be continuously powered by the ambient moisture.^[109] This innovative generator merged the processes of water absorption and desorption, utilizing a hygroscopic layer alongside an evaporative layer as illustrated in **Figure 6e(i,ii)**. Impressively, this device could produce a consistent voltage of $\approx 0.78 \text{ V}$ and a current of $\approx 7.5 \mu\text{A}$ for more than ten days under standard ambient conditions (**Figure 6e(iii)**). Moreover, the device's power output could easily be increased through serial and parallel configurations, enabling it to directly charge batteries or capacitors. This breakthrough technology represents a significant advancement toward generating continuous electricity from our environment, presenting a significant advancement in the pursuit of renewable energy solutions.^[109]

To further extend the applicability of moisture-driven generators over the long term, Zhao et al. introduced a bilayered MEG with exceptional environmental durability and long-term operation.^[105] The MEG features a bilayer architecture in which a surface-active material serving as the power generator is placed onto a hydrogel layer acts as a water reservoir. This design was able to minimize the device's dependence on external humidity levels by maintaining a consistent internal water gradient. By integrating an organohydrogel known for its excellent water retention and structural stability with 3D structured Mxene aerogels, the device demonstrated a power density of $24.8 \mu\text{W cm}^{-2}$.^[105]

3.2.2. Flexible Photovoltaic Energy Harvesters

Flexible photovoltaic devices are a promising alternative to conventional energy sources for certain applications where natural or synthetic light is abundant. As illustrated in **Figure 5g**, flexible solar cells that can be embedded underneath the skin or integrated into clothes offer a viable energy source for powering wearable and implantable devices.^[110] Various categories of solar cells have been investigated for wearable applications, including flexible perovskite solar cells.^[111–114] As an example, Lv et al.

created high-performance fiber-shaped organic solar cells employing nonfullerene-acceptor light harvesting materials.^[115] These innovative fiber-shaped cells reached efficiencies $\approx 9\%$ under AM 1.5G irradiation condition, which is typically 1000 W m^{-2} . Tholl et al. demonstrated that the daily energy requirement of a contemporary cardiac pacemaker, $\approx 10 \mu\text{W}$, can be fulfilled by a solar cell of 2.0 cm^2 implanted 3.0 mm beneath the skin, under midday clear sky irradiation for 11 min .^[116] Indoor irradiance reached 4 W m^{-2} , leading to a power output of $4 \mu\text{W cm}^{-2}$ for the subdermal solar cell, indicating an approximate light absorption and conversion efficiency of 1% within the cell. Furthermore, Song et al. reported that a solar cell implanted beneath a mouse's skin under AM 1.5G solar conditions can generate a peak power density of about 10 mW cm^{-2} .^[117] Additionally, Lu et al. found the power density for a solar cell positioned under 2 mm of skin and 2 mm of fat to be $\approx 17.37 \text{ mW cm}^{-2}$ under the same AM 1.5G conditions.^[118]

While solar cells hold excellent potential for WIMDs, their power output and conversion efficiency can significantly decline under conditions of low light and elevated body heat, particularly in small, implantable applications. However, results from recent publications for solar cells are normally under the standard test condition of AM 1.5G irradiations. The indoor light spectrum is often a combination of natural and artificial light, and the irradiance levels range between 0 and 100 W m^{-2} ,^[119] which is only 0.1% of AM 1.5G irradiation condition. Under such a typical indoor lighting condition, the power output of solar cells will be much lower compared with the standard experimental tests.

Moreover, the positioning of PV cells whether skin-mounted, cloth-integrated, or implanted greatly influences their power outputs. Additionally, factors such as implantation depth and size constraints in implantable applications affect the maximum energy they can capture.^[110] Hence, substantial challenges and opportunities lie ahead in advancing wearable and implantable photovoltaic cells to effectively meet the power demands of WIMDs summarized in Figure 7 and Table 1.

4. Wireless Energy Transfer Technologies

Unlike harvesting energy from the motion of the human body using TENGs and PENGs, wireless energy transfer techniques can deliver power from external energy sources, overcoming the risk of infection associated with wired connections of the energy harvesters. We will focus on four types of wireless energy transfer technologies that are promising for wearable and implantable medical applications, including inductive transfer, capacitive coupling, and ultrasound-induced energy transfer and harvesting. Table 2 shows some recent examples of wireless energy transfer techniques for medical applications. Such wireless energy transfer techniques offer another significant advantage in the control of power parameters such as current density, pulse width, frequency, and duty cycle.^[133,134]

4.1. Inductive Power Transfer

Inductive power transfer (IPT) (Figure 8a) is the most widely used wireless power transfer technology for applications with short

range or shallow tissue depth. The overall system comprises two inductive coils with one inside of the body and the other outside of the body to transfer power wirelessly. Voltage will be induced in the receiver coil due to electromagnetic induction when a sinusoidal current is placed on the transmitter coil.^[135] This method is notably efficient for transfers over a short distance, ranging from millimeters to a few centimeters, but its efficiency diminishes sharply with the transfer distance, rendering it less effective for long-range power transmission. IPT is commonly utilized in situations where the power source and the receiver must be well aligned and in proximity, such as in certain medical implant applications.^[136]

For powering implantable medical devices, Choi et al. demonstrated a bioresorbable temporary cardiac pacemaker that utilized wireless inductive power transfer for its operation.^[137] This unique cardiac pacemaker was successfully powered *ex vivo* on the mouse, the rat, and human cardiac tissue. It was designed to operate at a frequency of 13.5 MHz and the output reached 13.2 V upon contact with heart tissue. A distinctive characteristic of this pacemaker is its capacity to fully dissolve in biofluids over approximately three months, significantly diminishing the infection risks commonly associated with pacemaker replacement surgeries. The operation of implanted devices that function wirelessly and without batteries was demonstrated, which are gradually dissolved through biosorption as time progresses.

Sivaji et al. developed an innovative implantable peripheral nerve stimulation system that operates wirelessly without needing a battery, thereby eliminating the need for additional surgeries to replace batteries.^[138] As illustrated in Figure 8b(i), the system consists of three major components: an implanted pulse generator (IPG), a relay module outside the body and positioned directly over the IPG during stimulation, and a programmable module. The IPG, which is implanted directly on the nerve of interest, uses a near-field communication (NFC) tag for wireless communication and power harvesting. The power harvesting circuit outputs a maximum of 3 V , which is used to power the rest of the device. The 3 V output from the NFC tag is stepped-up to 12 V by a boost converter and then fed to the stimulator. The relay module is battery powered and provides wireless power to the IPG through inductive coupling at 13.56 MHz , a frequency that results in negligible absorption in the body. The team also demonstrated the operational performance, reliability, biocompatibility, implantation safety, and nerve stimulation efficacy of this system. In vivo tests were conducted to assess the device's long-term biocompatibility and safety. Five pairs of devices were successfully implanted in five dogs, with the devices on the right vagus nerve remaining unstimulated and those on the left nerve stimulated for 28 days . Each animal underwent at least $14\,000 \text{ s}$ of stimulation throughout the study. The operational amplifier voltage required to deliver 1.2 mA of current remained safely under the 12 V compliance voltage for the entire 28 days . Additionally, despite the animals' constant movement, the communication success rate exceeded 80% , except for the initial days when the relay module was not securely mounted, as shown in Figure 8b(ii). These results indicate its potential for effective nerve stimulation without the drawbacks associated with implanted batteries.^[138] However, the efficiency of IPG is influenced by various factors, including the distance between the implanted generator and the relay module, and the misalignment between them.

Table 1. Properties reported for energy harvesters with different functional materials for medical applications.

Medical application	Type	Material	Size	Output performance	Refs.
Neural stimulation	TENG	PTFE/Cu	16 × 12 × 2.5 mm ³	200 mV 20.8 μW cm ⁻³ (at 20 MΩ)	[120]
Cardiac pacemaker	TENG	PTFE/Al	39 × 61 × 0.99 mm ³	0.495 μJ 110 mW m ⁻² (at 100 MΩ)	[65]
Cardiac pacemaker	TENG	PFA/PVA-NH ₂	706.8 mm ²	4.9 μW cm ⁻³ (at 10 MΩ)	[66]
Cardiac pacemaker	TENG	POM/PTFE	1525.3 mm ³	2200 mW m ⁻³ (at 100 MΩ)	[67]
Peripheral nerve restoration	TENG	PVDF/ZNO/silicon rubber	1600 mm ²	509 V 72 mW m ⁻² (at 20 MΩ)	[68]
Cardiac pacemaker	PENG	PVDF/ZnO/rGO	1.5 × 1.5 cm ²	0.487 μJ 140 μW cm ⁻³ (at 1 MΩ)	[89]
Arterial pulse monitoring	PENG	PZT	1 cm ²	100 mV	[93]
Cardiac pacemaker	PENG	PMN-PT	10 × 25 cm ²	6.9 μW (at 400 kΩ)	[122]
Heart rate monitoring	PENG	MXene/black phosphorus	8 × 8 cm ²	6.94 mA cm ⁻² 2.22 mW cm ⁻²	[124]
Respiration sensor	Twistron harvester	CNT	360 μm diameter 47 mm long	250 W kg ⁻¹ 41.2 J kg	[16]
Gastric stimulator	Twistron harvester	CNT	360 μm diameter 47 mm long	37 mV 600 mW kg ⁻¹	[95]
Human motion monitoring sensor	Electromagnetic generator	Spherical magnet	11.97 cm ³	74 mW peak power 0.73 mW cm ⁻³	[53]
Heart monitoring	Electromagnetic generator	Neodymium magnet (Nd ₂ Fe ₁₄ B) magnetic yarn	5 × 30 cm ²	3197 mW m ⁻² (at 750 Ω)	[125]
Heart rate monitoring	Electromagnetic generator	Neodymium-iron-boron (NdFeB) nanomagnetic (Magnenequench)	4 × 6 cm ²	0.63 mA cm ⁻² 6.67 W m ⁻² (at 180 Ω)	[127]
Body heat harvesting	Thermoelectric generator	P and n type bismuth telluride	25.4 × 25.4 × 9.5 mm ³	35 μW cm ⁻² (at 2.5 °C temperature difference)	[129]
Body heat harvesting	Thermoelectric generator	Carbon nanotube fiber	0.86 m ²	70 mW m ⁻² (at 44 K temperature difference)	[130]
Wearable motion sensor	Moisture-driven energy generator	MXene/PAM	3 cm ²	600 mV 1160 μA cm ⁻² 24.8 μW cm ⁻²	[105]
Cardiac pacemaker	Photovoltaic energy harvester	GaN/P/GaAs	6.8 mm ²	10 mW cm ⁻²	[117]
Cardiac pacemaker	Twistron harvester	CNT	61 turns cm ⁻¹	1.42 W kg ⁻¹ (peak power at 60 beats per minute) 0.338 μJ (1 Hz, 20% strain, four connected in series)	[96]

Table 2. Properties reported for energy transfer technologies with different functional materials.

Type	Element	Material	Frequency	Dimension	Output	Range	Refs.
Inductive power transfer	Two inductive coils	Tungsten-coated magnesium	13.5 MHz	Tx coil: 64 mm diameter Rx coil: 25 mm diameter	13.5 V	<17 cm	[137]
Inductive power transfer	Two inductive coils	Metal	13.56 MHz	Tx: 6 cm diameter Rx: 1.6 × 1.6 mm	12 V 1200 μA	2 cm	[138]
Capacitive power transfer	Four conductive plates	Tx: Copper Rx: PAAM hydrogel/NaCl salt	4.4 MHz	Tx: 50 × 70 mm Rx: 20 × 40 mm	4 mA	2 mm	[140]
Radio frequency wireless power transfer	Antenna	Copper	13.56 MHz	Tx: 20 × 30 cm/16 × 25 cm Rx: 5.5 mm radius	4 W	8 cm	[142]
Radio frequency wireless power transfer	Antenna	Copper	13.56 MHz	Rx: 10 × 5 mm	12 W	2.5–7.5 cm	[143]
Radio frequency wireless power transfer	Antenna	Copper	13.56 MHz	Tx: 25 × 15 cm Rx: 0.9 cm ²	12 mW	3 cm	[149]
Ultrasound-induced power transfer	An ultrasound transmitter and an ultrasound receiver	Lead-free piezoelectric 1–3 composite	304 kHz	Receiver: 1 × 1 mm ²	45 mW cm ⁻²	20 mm	[150]
Ultrasound-induced power transfer	An ultrasound transmitter and an ultrasound receiver	PVDF/BZT-BCT@PDA	1 MHz	Receiver: 1.5 × 1.5 cm ²	0.16 mW cm ⁻²	2–10 cm	[134]
Ultrasound-induced power transfer	An ultrasound transmitter and an ultrasound receiver	PFA/copper/gold	20 KHz	Receiver: 4 × 4 cm ²	1.93–2.4 V 98.6–156 μA	5–10 mm	[148]

Consequently, a significant challenge remains in improving the power transfer efficiency of IPTs in the presence of misalignments between coils, especially when one of the coils is attached to the continuously moving internal body organ.^[139] Moreover, metamaterials are promising route to reducing the size of the coils, miniaturizing IPTs, while maintaining the efficiency.

4.2. Capacitive Power Transfer

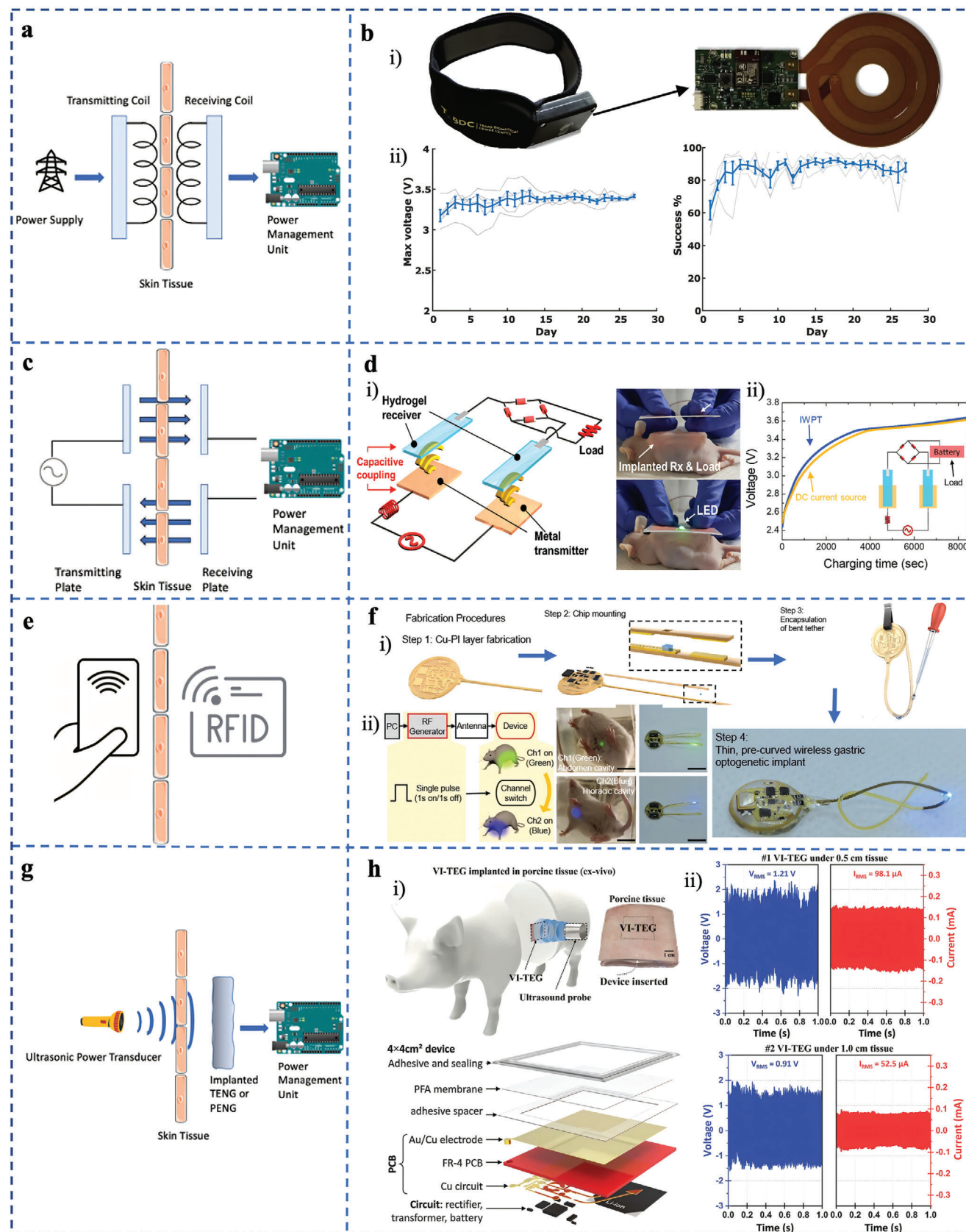
Capacitive power transfer (CPT) (Figure 8c) delivers power by using an electrostatic induction between two coupled metallic plates acting as power transmitter and power receiver, respectively.^[140] Kim et al. introduced an ionic wireless power transfer (IWPT) system, leveraging capacitive coupling through ion conductive plates to transmit power. This innovative system, designed to operate on input signals with an amplitude of less than 10 V, ensures safety even when transferring power to implants. The capacitive coupling was effectively demonstrated using various gap-filling materials, including both dielectric substances and electrolytes. This capability allows the IWPT system to deliver power to subcutaneous sites in a mouse through the skin, showcasing the system's potential for noninvasive power transfer to implants (Figure 8d(i)). The charging curve was represented by the blue line in Figure 8d(ii). The battery's theoretical capacity is 13.6 mAh, and the current measured at the receiving end was ≈1.4 mA. For comparative purposes, the battery was also charged using a wire-based system where a direct current source provided a steady current of 1.4 mA (yellow line). Both curves indicate that the current measured was effectively stored in the battery by the IWPT system.^[140]

The advantage of CPT is its higher misalignment tolerance compared with inductive coupling. However, the current system is too bulky for implantable situations as it requires four large plates to achieve the necessary power transfer. Therefore, there is a need to reduce the size of capacitive coupling while maintaining the power transfer performance, which will greatly enhance its suitability for implantable use.

4.3. Radio Frequency Wireless Power Transfer

Devices employing radio frequency (RF) for wireless power transfer can transmit energy over distances greater than those achievable by IPT (Figure 8e). The efficiency of this power transmission is influenced by factors such as the separation between the devices, surrounding conditions, and the operational frequency. Unlike IPT, RF power transfer does not require precise alignment or proximity between the transmitter and receiver. Incorporating compact components capable of RF power transfer and control facilitates the observation of animals in their natural settings, free from the limitations imposed by physical connections like electrical wires.^[141]

Wireless devices that utilize RF for power are commonly deployed to energize microscale light-emitting diodes (μLEDs) for optogenetic applications. Kim et al. have developed a resilient, multifunctional, and wireless solution designed to facilitate the optogenetic activation of peripheral nerves within body organs efficiently.^[142] The fabrication process for manufacturing the device is depicted in Figure 8f(i). This compact device, which can be



completely implanted, features a flexible and soft tether aimed at directing a μ LED to specific organ locations. Through an innovative production technique, they crafted a durable tether that houses a μ LED, enabling sustained (>1 month) and close interaction with peripheral nerve endings in mice that move freely (Figure 8f(ii)). This setup included an analogous, front-end circuit for RF energy capture measuring 5.5 mm in diameter and 1 mm in thickness and an electrical wire that directs the current to a μ LED. This device captured RF energy from a wireless RF-power system situated remotely, transformed this RF energy into light, and illuminated it on precise areas within the stomach.^[142]

Samineni et al. introduced a fully integrated optoelectronic device powered by RF, featuring a flexible design tailored for optical activation of the spinal cord. This system operated within the scope of an external dual-loop antenna, which was strategically placed around the cage's edge, facilitating wireless power transfer. At the device's core, a Schottky diode mounted on the tip of the probe efficiently converted the received RF signals into electrical power for the micro-LED. Additionally, a capacitor (40 pF) located at the base of the probe was crucial for achieving the impedance match needed for the system's effective functioning.^[143]

It has been observed that the range of devices wirelessly powered by RF signals is notably constrained, yet they do not limit the movements of living creatures.^[144] Furthermore, variations in magnetic flux density between the near-field and far-field ranges present distinct challenges for RF energy harvesting. In the near field, achieving optimal impedance matching and precise antenna alignment remains a significant hurdle for designers. In the far-field, due to the lower magnetic flux density, gathering enough energy to activate the circuit with a far-field RF harvester proves difficult, especially as start-up thresholds vary across different CMOS technologies.^[110]

4.4. Ultrasound-Induced Power Transfer

Ultrasonic energy transfer and communication employ traveling ultrasonic waves to transmit energy with adjustable output power and longer transmission distance (Figure 8g). It has several advantages such as deeper penetration and high-level safety for biomedical applications. The attenuation of ultrasound power in biological tissue is much smaller when compared with other electromagnetic-based wireless energy transfer technologies, i.e., it can have a deeper travel depth through the tissue with less energy loss.^[145] The US Food and Drug Administration settles the limit for ultrasound intensity for peripheral vascular $\approx 720 \text{ mW cm}^{-2}$ and cardiac $\approx 430 \text{ mW cm}^{-2}$.^[146] Piezoelectric materials are usually used as transceivers to combine with ultrasound power transmission to form ultrasound-induced wire-

less energy harvesting systems for implantable medical devices. Jiang et al. in 2019 proposed a flexible device made from piezoelectric materials which can be driven by the ultrasonic wave to produce continuous voltage and current.^[147] In 2021, Chen et al. demonstrated a piezoelectric thin film-based nanogenerator remotely driven by programmable ultrasound pulses, which could directly stimulate the peripheral nerves.^[134] The performance of this battery-free neural stimulator was validated through sinusoidal pulse waveforms designed with various pulse widths and intervals, programmed from ultrasound input parameters. Surprisingly, the voltage output of these piezoelectric thin film-based neural stimulators remained consistent for two months after postimplantation in rats.

Furthermore, combining ultrasound induction and TENG has been reported as a promising approach for implantable applications. Hinchet et al. reported an ultrasound-induced high-frequency vibrating TENG, demonstrating the feasibility of recharging the battery of small implants through pig tissue (Figure 8h(i)). Their device was tested at depths of 5 and 10 mm. At the depth of 0.5 cm, the device produced output signals exceeding 2.4 V and 156 mA, as shown in Figure 8h(ii). The observed reductions in voltage and current were attributed to the attenuation of ultrasound signals. Furthermore, when positioned 1.0 cm deep under layers of tissue including skin and fat, the device generated output signals greater than 1.93 V and 98.6 mA. The prototypes demonstrated the ability to generate power in the milliwatt range, which is adequate for recharging capacitors and lithium-ion batteries.^[148]

5. Energy Storage

The energy harvested from various sources needs to be stored for future use by wearable and implantable medical devices, which require energy storage solutions that are not only reliable and long-lasting, but also biocompatible and safe for on- or in-body use.

Flexible supercapacitors are emerging as an effective solution for the energy storage demands of wearable and implantable biomedical devices. They offer superior power densities compared to traditional batteries and excel in energy storage through mechanisms like ion adsorption and rapid surface redox reactions. Advantages include improved safety, quick charging and discharging, and longer lifespan. Although they have lower energy density than batteries, their higher power density, fast recharge rates, and reduced toxicity make them ideal for medical applications, particularly when paired with energy harvesting and wireless power transfer technologies.^[151,152] Rechargeable batteries, particularly lithium-ion, are the primary choice for WIMDs due to their high energy density and stable performance.^[31]

Figure 8. Energy transfer technologies. a) Working principle of inductive power transfer. b) (i) Relay module PCB with the flex coil that is used to power the implantable neural stimulator. (ii) Outcomes of long-term biocompatibility assessments: Voltage needed to administer 1.2 mA of current across five animals and success rate of IPG communication for the five animals. Adapted with permission.^[138] Copyright 2019, Elsevier. c) Capacitive power transfer mechanism. d) (i) A capacitive coupling power transferring system implanted in a mouse to power green LEDs. (ii) Charging curve of a battery through implantable wireless power transfer systems and DC power source. Adapted with permission.^[140] Copyright 2020, American Chemical Society. e) Working principle of RF power transfer. f) (i) Fabrication procedure of the device. (ii) Remote control for stimulating multiple organs in rats. Adapted with permission.^[142] Copyright 2021, The Author(s). g) Working principle of ultrasound-induced wireless power transfer. h) (i) Illustration chart of wireless power transfer devices implanted in the porcine. (ii) Voltage and current generated by the device implanted at 0.5 and 1 cm under the porcine tissue. Adapted with permission.^[148] Copyright 2019, The American Association for the Advancement of Science.

Table 3. Table of wearable and flexible supercapacitors and batteries reported recently.

Materials	Process	Power density [mW cm ⁻²]	Energy density [μWh cm ⁻²]	Refs.
Cu ₂ O/Cu(OH) ₂	Metal plated coating	9.5	1.74	[155]
Cu ₂ O/Cu(OH) ₂ /graphite	Metal plated coating	20.0	8.81	[155]
MoO _x /Mo	Electrochemical oxidation	2.53	15.64	[156]
Crystalline tetra-aniline	Solution self-assembly	0.82	80.3	[157]
Sericin/reduced graphene oxide	Sequential cross-linking	0.026	0.014	[158]
Activated carbon/gold	Annealing	0.78	10.86	[159]
PEDOT:PSS	Solution drop casting	0.031	0.74	[160]
Mg-MoO ₃	Slurry pasting	196	4.70	[161]
MnO ₂ /CNT	Electrodeposition	0.819	84.18	[162]

Recently, zinc-ion batteries have gained popularity as a sustainable and safer alternative, offering benefits such as the abundance and affordability of zinc, making them more suitable for medical applications. Additionally, the use of aqueous electrolytes significantly increases safety by reducing the fire and explosion risks associated with lithium-ion batteries.^[153]

Nevertheless, the energy/power densities of wearable or implantable rechargeable batteries/supercapacitors remain a limiting factor for the miniaturization of the energy source. Innovative research in new material chemistries and battery designs is critically needed for miniaturized, biocompatible battery systems that are not only high-performing but also seamlessly integrate with the ergonomic and physical requirements of medical devices.^[154]

Wearable and implantable energy storage devices are grouped into four categories: biocompatible energy storage devices, microenergy storage devices, stretchable/deformable energy storage devices, biodegradable/bioabsorbed energy storage devices, and high-performance energy storage devices. Each category addresses a unique set of challenges and requirements, underscoring the manuscript's comprehensive approach to advancing energy storage solutions in the medical field. **Table 3** illustrates the table of recently reported wearable supercapacitors and batteries, mapping the performance of various materials by energy density (in μWh cm⁻²) against power density (in mW cm⁻²) on logarithmic axes. Most supercapacitors have an energy density ranging between 1 to 100 μWh cm⁻². While some achieve energy densities up to 10⁴ μWh cm⁻², the trade-off is a lower power density compared to their peers. Overall, from an energy storage perspective, the performance of wearable energy storage devices still falls short when compared to their traditional counterparts.

5.1. Biocompatible Energy Storage Devices

Biocompatibility refers to the ability of a device to safely function within the human body. A biocompatible material does not provoke adverse reactions or long-term changes in the body, allowing it to coexist with biological systems without causing harm or toxicity. The assessment of biocompatibility is essential in the development of medical devices, as it ensures that the materials used are compatible with the body's tissues and biological processes, minimizing the risk of rejection, inflammation, or other negative responses.^[163] A notable advancement in this domain is the emergence of open-system power sources. By utilizing body

fluids as natural electrolytes, these systems circumvent the need for potentially harmful encapsulated electrolytes, marking a significant step forward in biocompatible energy solutions.

Given their nontoxic nature, natural polymers hold significant promise for biomedical applications, including implantable devices. However, the long-term durability of flexible or implantable energy storage devices is a major factor as continuous deformation may lead to electrode damage.^[164] The development of self-healable, biodegradable energy storage devices based on natural polymers addresses these concerns.^[165] Hsu et al. presented a self-healable and biodegradable hydrogel supercapacitor using natural polymers like tannic acid, gelatin methacrylate, and cellulose nanocrystals.^[166] This device was further enhanced with polyaniline (PANI) and reduced graphene oxide through in situ polymerization, presenting a flexible, self-healing supercapacitor, aligning with sustainability goals and the demands of the medical electronics market.^[166]

Building on these foundational principles, Tong et al. developed a supercapacitor using crystalline tetra-aniline as the electrode, which is self-repairable and biocompatible.^[157] The self-healing capability of the device stems from the strategic integration of polyethylene glycol (PEG) with crystalline tetra-aniline to form a self-repairing electrode. This design exploits the reversible hydrogen bonds in PEG, enabling the electrode material to autonomously mend itself after sustaining physical damage. Its resilience is further augmented using a ferric-ion cross-linked sodium polyacrylate gel electrolyte, which possesses inherent self-healing properties due to its dynamic ionic cross-linking that can spontaneously reform post-damage. This innovative approach ensures that the device can preserve its functionality and structural integrity even after undergoing cuts or tears, thereby significantly extending its useful life and reliability for wearable and implantable electronics applications.^[157]

Additionally, body fluid, tears, and sweat can serve as biocompatible electrolytes. For instance, Chae et al. developed a composite material consisting of MnO₂ nanoparticles and multiwalled carbon nanotubes for the positive electrode, paired with phosphidated activated carbon to enhance biocompatibility at the negative electrode.^[167] This approach uses body fluids, rich in various ions like Na⁺, K⁺, Ca²⁺, Cl⁻, and HCO³⁻, as the electrolyte in an open system, thereby minimizing leakage risks and circumventing the issues associated with toxic electrolytes in traditional energy storage devices. This method shows a promising path toward maintaining capacitance with minimal loss, even

in an open system.^[167] Furthermore, Yun et al. have developed flexible aqueous batteries for smart contact lenses that utilize tears as the electrolyte, presenting a safer alternative to traditional batteries that could cause severe eye injuries if damaged. These batteries incorporate nanocomposite electrodes embedded in a UV-polymerized hydrogel, serving both as a contact lens and an ion-permeable barrier (Figure 9a(i,ii)). Demonstrating a discharge capacity of 155 μAh with an electrolyte composition of human tears, these batteries can sufficiently power low-energy electronics, validated for mechanical stability and compatibility with standard lens care solutions, highlighting their practicality and safety. Long-term cycling performance tests showed that the capacity retention was superior to performance in tears and that the Coulombic efficiency was $\approx 97.5\%$ (Figure 9a(iii)).^[168] Additionally, Bandodkar et al. have developed a sweat-activated battery technology for epidermal electronics, overcoming the limitations of conventional batteries that pose risks due to their hazardous materials and rigid structures. Incorporated into a soft, microfluidic system, this technology allows for the embedding of electronic modules for power management and wireless communication. This advancement has been validated through human trials, successfully powering devices that monitor heart rate, sweat chloride, and pH values.^[169]

5.2. Microenergy Storage Devices

In the field of bioelectronics and medical devices, which includes both implantable and wearable technologies, the trend toward miniaturization without sacrificing functionality has intensified the focus on microenergy storage systems like microbatteries and supercapacitors. The key advantage of these microscale energy solutions lies in their compactness, which facilitates the creation of more discreet and comfortable wearable devices, as well as less invasive implantable devices, without compromising their operational functionality. Therefore, the advancement of microenergy storage devices is crucial, demanding innovative design and fabrication approaches that are in tune with the evolving demands of bioelectronics. This ensures that the devices remain effective user-friendly, meeting the critical need for both convenience and reliability in medical applications.

To this end, traditional film-type supercapacitors made of hard materials may pose limitations for implantation due to their bulkiness and rigidity, potentially impeding tissue, and organ movement in daily activities. To address this issue, Sim et al. introduced a flexible, fiber-type implantable micro-supercapacitor with a slender diameter of only 80 μm , designed for in vivo energy storage. Constructed from biocompatible materials PEDOT:PSS with ferritin nanoclusters embedded in multiwalled carbon nanotube sheets, this micro-supercapacitor exhibits exceptional flexibility and is envisioned as a feasible implantable device. Its fiber-like form allows for implantation within narrow bodily spaces, such as organs, tissues, and blood vessels, and it can even be utilized as a suture in medical procedures.^[170]

In addition to fiber-shaped devices, Gao et al. introduced an edible micro-supercapacitor (EMSC) tailored for noninvasive diagnostics and applications inside the body, employing components found in food as its main materials. This strategy overcomes the challenges and health risks associated with conventional biocom-

patible materials and maintains the electrode structure's durability across various physical stresses. The EMSC features ingestible and biologically safe electrodes and electrolytes, making it suitable for human consumption. Its robust mechanical properties and versatility enable the device to conform to different shapes, including flat and curved surfaces like human skin. The EMSC achieves a significant energy storage capacity of 10.86 $\mu\text{Wh cm}^{-2}$ and a power output of 0.78 mW cm^{-2} , sufficient to power a red LED when two EMSCs are connected in series. Additionally, its potential for integration into the casing of a medical pill showcases its capability to energize capsule endoscopy within a synthetic stomach acid setting, underscoring its suitability for direct in-body monitoring and diverse biomedical uses.^[159]

5.3. Stretchable/Flexible Energy Storage Devices

Integrating the inherent softness and flexibility of human tissues into the design of medical devices offers significant advantages. Stretchable energy storage devices, designed with materials that emulate the flexibility of human skin, hold promising potential for bioelectronics, particularly in the domain of health monitoring. These devices are engineered to seamlessly integrate with the body's natural movements, offering a more comfortable and less intrusive option for continuous health tracking. Their adaptability and durability under deformation make them ideal for wearable technologies that require consistent performance over time, enhancing the user experience in medical monitoring applications.^[171] Developing such energy storage devices requires a multidisciplinary approach, focusing on biocompatibility and mechanical properties, alongside innovative design and manufacturing techniques.

A flexible and deformable electrolyte plays a crucial role in designing supercapacitors that exhibit both high elasticity and impressive electrochemical capabilities.^[172] The ideal flexible electrolyte would feature excellent ionic conductivity, remarkable electrochemical stability, strong biocompatibility, and notable flexibility. Various types of electrolytes including liquid electrolytes,^[173] solid-state electrolytes,^[174] and gel electrolytes^[175] are extensively utilized in most flexible supercapacitors. Li et al. showcased a hydrogel electrode with a fiber-like structure, created through the self-assembly process of graphene oxide (GO) and PANI hydrogels, combined with a poly(vinyl alcohol) (PVA)/sulfuric acid gel electrolyte.^[176] This innovation led to the development of an all-gel-state supercapacitor that stands out for its exceptional flexibility, formability, and enhanced electrochemical performance.

Furthermore, Ye et al. developed an ultrasoft and deformable hydrogel-based battery to address the need for power sources that closely mimic the mechanical properties of biological tissues (Figure 9b(i)). These all-hydrogel batteries display a low Young's modulus of 80 kPa, making their mechanical characteristics compatible with that of skin and vital organs like the heart. The all-hydrogel batteries demonstrated remarkable durability, showing almost no loss in capacity after 5000 bending cycles at 180 °C and stretching by 30% strain. These soft batteries also retained stable capacities after being twisted at 90° for 5000 cycles and at various other angles. Additionally, even under severe shearing deformation over 5000 cycles, the capacities remained

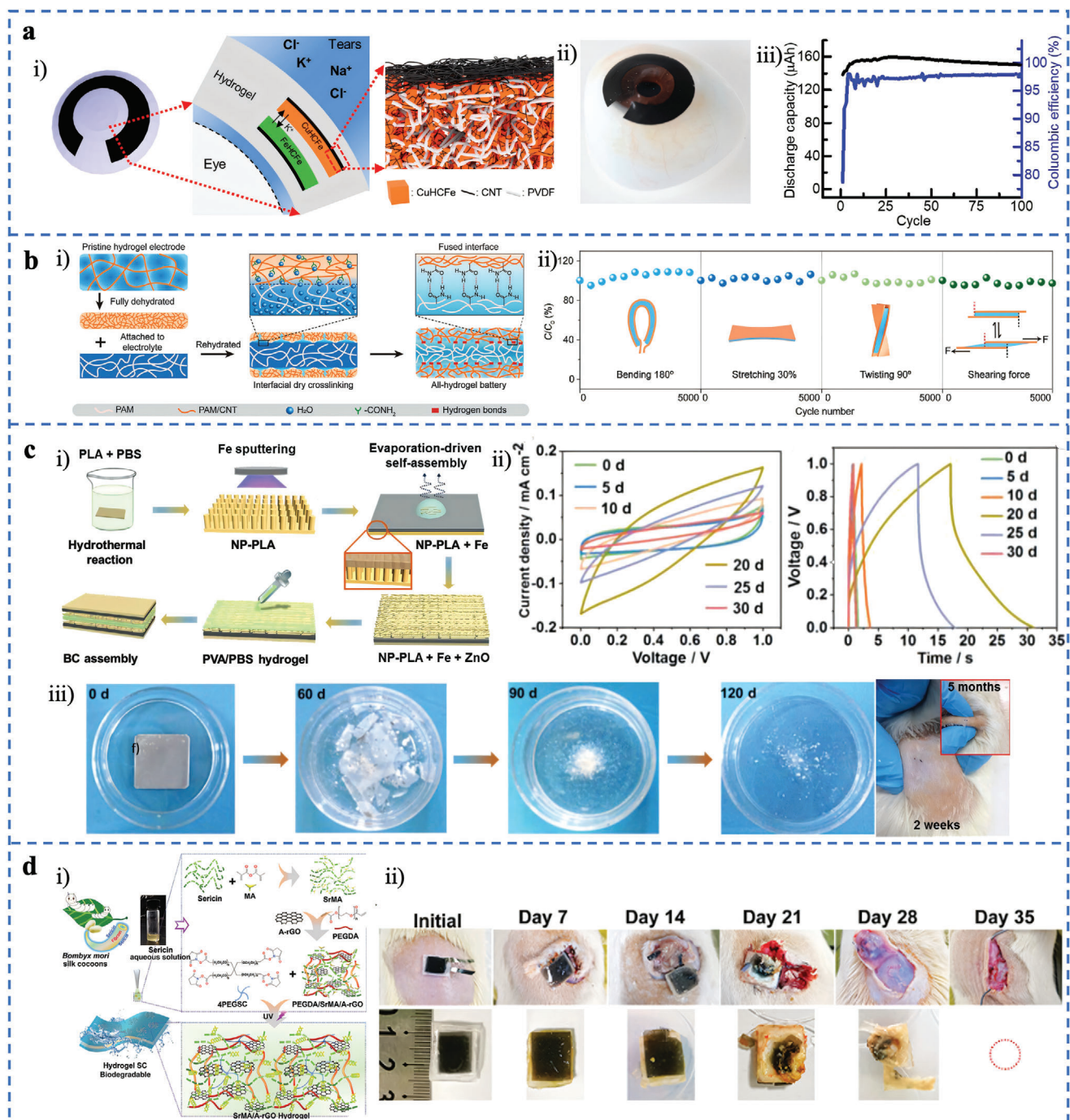


Figure 9. Flexible and stretchable rechargeable batteries. a) (i) Illustration chart of the battery made of porous electrodes and hydrogel. (ii) Battery placed on a fake eye model. (iii) Cyclic durability and Coulombic efficiency of the battery within the cleaning solution. Adapted with permission.^[168] Copyright 2021, American Chemical Society. b) (i) The fabrication method for the all-hydrogel battery using interfacial dry cross-linking. (ii) All-hydrogel based batteries under bending, stretching, twisting, and shearing tests for 5000 cycles. Adapted with permission.^[177] Copyright 2021, John Wiley and Sons. c) (i) Method of fabricating the supercapacitor through evaporation-driven self-assembly technology on an NP-PLA support substrate. (ii) Long-term electrochemical performance test at 37 °C. (iii) Degradation test of the supercapacitor in a cell-culture dish and images of implanted site containing the device before and after degradation over various periods. Adapted with permission.^[181] Copyright 2019, The Author(s). d) (i) Production method and use of the supercapacitor featuring a SrMA/A-rGO hydrogel electrode. (ii) Photographs of degradation assessment for implant in the subcutaneous area of SD. Adapted with permission.^[158] Copyright 2023, John Wiley and Sons.

consistent, thereby preventing any error of the batteries due to external friction (Figure 9b(ii)). Their application in wearable and implantable devices has proven their high stability and biocompatibility, positioning them as an optimal solution for devices requiring seamless integration with biological tissues.^[177]

Besides, fiber-based batteries and supercapacitors are garnering significant interest for their adaptability in wearable technologies. Pullanchiyodan et al. have introduced an innovative method for creating fabric-based supercapacitors for wearable devices, employing metal-coated textiles combined with a harmless polyvinyl alcohol gel electrolyte.^[155] This study represents a significant advancement in wearable supercapacitors through the innovative use of metal coatings on textiles, which serve dual purposes as both the functional layer and the current collector, resulting in a substantial enhancement of the electrochemical performance. Additionally, the supercapacitor maintained its capacitance over 5000 charge/discharge cycles, highlighting its durability and reliability for long-term application in wearable technology.^[155]

5.4. Biodegraded/Bioabsorbed Energy Storage Devices

The environmental footprint of traditional battery components is a significant concern due to their long decomposition times, which exceed a century when left in natural settings, alongside the toxic emissions and substantial CO₂ produced during incineration.^[178] The non-degradable synthetic substances within batteries pose serious threats to biological systems, potentially causing organ damage or even fatality in living beings. Given the surge in battery usage, the environmental influence of these materials demands urgent attention. To counter the growing environmental impact and enhance sustainability, there is a pressing need for innovative solutions that reduce the ecological risks tied to escalating battery production levels. Efforts are underway to incorporate biodegradable^[179,180] and bioresorbable^[181] substances as electrodes in standard primary battery setups, offering a partial solution by diminishing the overall accumulation of battery waste through their comparatively rapid degradation.

Pal et al. have introduced microfabricated supercapacitors that are both biocompatible and degradable, crafted from protein-based composites for both the electrodes and the flexible substrate.^[182] This device, primarily made of proteins and agarose polysaccharides, is designed to be absorbed by the body, making it ideal for temporary bioelectronic applications. Additionally, Li et al. introduced a fully bioabsorbable capacitor (BC) that holds potential as an energy storage device for both in vitro liquid environments and in vivo implantable medical devices (Figure 9c(i)).^[181] As shown in Figure 9c(iii), the biodegradability and real-time changes of the BC were evidenced by immersing it in PBS at 37 °C for four months. Initially, the BC maintained its structural integrity. Over subsequent immersions, the rectangular shape of the current and voltage curves progressively changed to an inclined shuttle-like shape. The symmetric curves became asymmetric, with a rapid voltage drop occurring along the discharging curves on the 20th and 25th days (Figure 9c(ii)). This change could be attributed to the increased distance between electrodes, partial corrosion of the electrodes, and weakened contact between the active material and electrode due to prolonged

immersion in PBS. These BCs could power 15 green LEDs immediately upon implantation in rats. Crucially, after serving its purpose, the BC can be completely degraded and absorbed by the organism, offering a sustainable energy solution for future implanted medical devices without necessitating secondary surgery or imposing financial strains.

Furthermore, Lv et al. have crafted a degradable supercapacitor implant by featuring an innovative hydrogel-based electrode. This electrode is produced via a unique process that forms a multinet network conductive structure with aminated-reduced-graphene-oxide-and-methacrylic-anhydride-modified sericin (SrMA/A-rGO) (Figure 9d(i)), bound together with four-arm polyethylene glycol succinimide carbonate and polyethylene glycol acrylate. On day 28, residuals of the implant were visible beneath the skin, with the decomposition product completely vanishing by day 35 (Figure 9d(ii)). Its utility is underscored by its capability to energize a light-emitting diode and, importantly, to kickstart a non-beating heart, indicating its value as a power source for essential medical uses like temporary pacemakers.

5.5. High-Performance Energy Storage Devices

With the rapid advances in active medical devices, the demand for wearable and implantable energy storage solutions has reached unprecedented levels. High performance refers to high power density for supercapacitors and high energy density for batteries. A high power density ensures quick bursts of energy, suitable for peak demands in device operation or emergency medical interventions. Inman et al.^[183] reported the development of MXene textile supercapacitors, utilizing Ti₃C₂T_x as the active material, tailored for real-world wearable electronics applications. By integrating these supercapacitors in a series via a stacked design, they achieved a notable energy density of 0.401 mWh cm⁻² and power density of 0.248 mW cm⁻², with an areal capacitance of 146 mF cm⁻² at a discharge current of 0.16 mA cm⁻², using a 5-cell configuration over a 25 cm² area with an MXene loading of 24.2 mg cm⁻². This MXene-based device successfully powered a temperature monitoring system with wireless data transmission for 96 min, demonstrating the practicality of MXene supercapacitors in powering peripheral electronics for wearable applications, thanks to their high current density handling capability.^[183] Moreover, Manjakkal et al. reported a wearable supercapacitor utilizing sweat as an electrolyte and PEDOT:PSS coated on a cellulose/polyester cloth as the active electrode, which demonstrated a specific capacitance of 8.94 Fg⁻¹ (10 mF cm⁻²) at 1 mV s⁻¹ with artificial sweat, showcasing energy densities of 1.36 and 0.25 Wh kg⁻¹, and power densities of 329.70 and 30.62 W kg⁻¹ with artificial and real human sweat, respectively.^[160]

High energy density allows for longer device operation on a single charge, essential for continuous health monitoring/regulating and critical medical applications. For high-energy density devices, metal-ion batteries such as lithium-ion batteries (LIBs) have attracted considerable attention in this area. For instance, Zhang et al. reported a high-energy density lithium-ion microbattery (LIMBs) by utilizing a scalable screen-printing technique to fabricate multilayer LIMBs with highly conductive and mechanically stable inks. The as-developed device exhibits a robust cross-linked conductive network with superior electrical

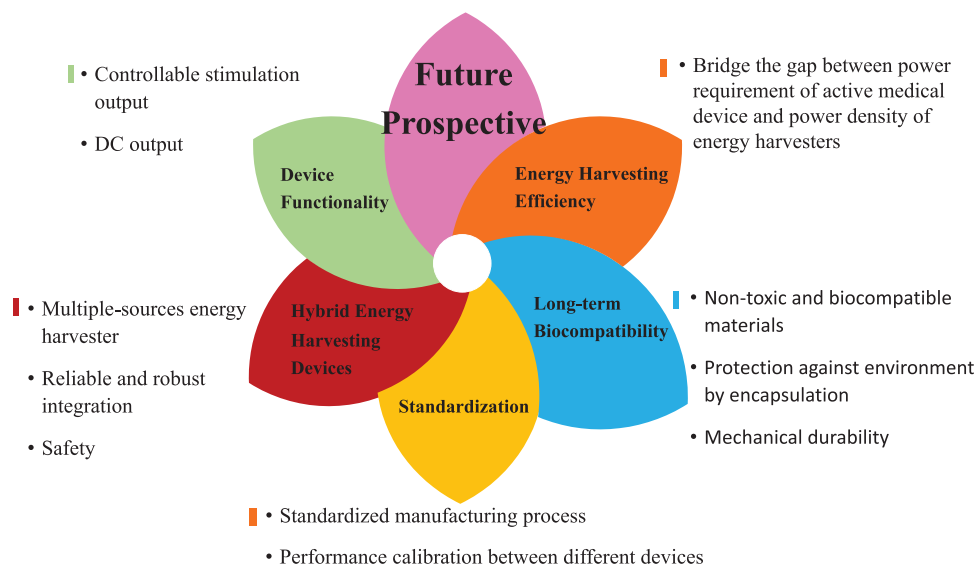


Figure 10. Challenges and future opportunities.

conductivity ($\approx 7000 \text{ ms cm}^{-1}$) and effective lithium-ion mobility. As a result, the LIMBs demonstrated an outstanding areal capacity of $398 \mu\text{Ah cm}^{-2}$ and an impressive areal energy density of $695 \mu\text{Wh cm}^{-2}$, outperforming most existing LIBs.^[184]

In addition to metal-ion batteries, it is always desirable for a supercapacitor to achieve high power density without significantly losing energy density. To this end, Zhou et al. reported a high-capacitance, foldable supercapacitor, achieving an impressive areal capacitance of 56 mF cm^{-2} and volumetric capacitance of 11140 mF cm^{-3} at 0.5 mA cm^{-2} .^[185] By integrating vertically grown graphene nanosheets (VGNs) with MnO_2 on nickel wire substrates, they developed a hybrid electrode that offers an energy density of $7.7 \mu\text{Wh cm}^{-2}$ and a maximum power density of 5 mW cm^{-2} , metrics that far exceed those of current MnO_2 /VGNs-based supercapacitors. These figures not only far outperform the volumetric capacitance and energy density of existing wire-shaped supercapacitors by ≈ 25 and 39 times, respectively, but also improve the areal energy density by 400% over the best state-of-the-art MnO_2 /VGNs supercapacitors. Furthermore, the supercapacitor demonstrates exceptional foldability, retaining high capacity even when molded into various shapes or bent to different curvatures, making it a highly viable option for next-generation wearable devices.^[185] Another work from their group further extended the energy density of supercapacitors, where an ultrahigh MnO_2 mass loading of up to 50 mg cm^{-2} on CNT electrode was achieved via the hierarchical design.^[162] This design leverages the high specific surface area ($\approx 120 \text{ m}^2 \text{ g}^{-1}$), excellent electrical conductivity, and robust mechanical properties of CNT mats to produce binder-free electrodes with an ultrahigh areal capacitance reaching 5000 mF cm^{-2} and a mass efficiency of 98%. The resulting flexible supercapacitors exhibit an areal capacitance of 947 mF cm^{-2} at 1 mA cm^{-2} and excellent stability under bending.^[162]

Efforts in lithium-ion battery research have pushed these devices close to their theoretical performance limits, particularly concerning electrode materials. Recently, lithium–sulfur (Li–S) battery has emerged as a promising successor. Comprising a sulfur cathode and a lithium anode, the Li–S battery leverages the

multielectron conversion electrochemistry between elemental sulfur and lithium. This interaction delivers significantly higher specific energy compared to conventional lithium-ion batteries, making Li–S batteries an exciting frontier for energy storage in medical devices and beyond. For instance, Chen et al. reported a 3D-printed Li–S battery by utilizing 3D printing techniques.^[186] They employed a graphene/phenol formaldehyde resin paste as the ink for 3D printing, which, after curing, endowed the cathode skeleton with robust mechanical strength. This material, along with the use of a classical SiO_2 template method for crafting a porous cathode skeleton, was instrumental in achieving an unprecedented active material loading of $\approx 10.2 \text{ mg cm}^{-2}$. With a conductive 3D framework and the associated high efficiency ion and electron transport pathways, the batteries exhibit a remarkable specific capacity of 505.4 mAh g^{-1} over 500 cycles.

One major issue of Li–S battery is the sulfide shuttle effect, where the dissolution of lithium polysulfides into the electrolyte causes their migration between the cathode and anode. Consequently, it leads to continuous loss of active sulfur material, reduced capacity and efficiency, and degradation of the electrode materials, shortening the battery's lifespan. Alhaji et al. demonstrated a technique for fabricating a freestanding interlayer of laser-scribed graphene that significantly reduces polysulfide movement in Li–S batteries. This technique resulted in a notable specific capacity (1160 mAh g^{-1}) and remarkable cycling stability, with a capacity retention of 80.4% after 100 cycles.^[187]

6. Challenges and Future Opportunities

Energy harvesters for WIMDs can enhance patient comfort by reducing the size of the power source and eliminating the need for surgical battery replacements. However, achieving clinical applications faces numerous challenges. Most generally, for all candidate harvester systems, energy harvesting efficiency, lifetime, and safety of energy harvesters within the human body are critically important concerns. Also, system development is needed for storing the harvested energy and determining when

it should be delivered to power WIMDs. Despite significant progress in harvesting technologies, further advancements or new approaches are needed to meet the growing requirements for device functionalities.^[79,188–191] Some of the challenges and future opportunities for energy harvesters are summarized in **Figure 10**. The most important of which is to bridge the gap between the power requirements of active medical devices, including their information transmission capabilities, and the power density of energy harvesters that can be achieved by using available energy sources (whether mechanical energy, thermal energy, light energy, and moisture-based energy generators).

Moreover, **Table 4** shows a comparison of advantages and disadvantages among different energy harvesters, wireless energy transfer devices, and energy storage devices. Batteries and supercapacitors remain the primary choices of energy storage sources. However, even there is demand for smaller size, flexibility, biocompatibility, and higher power density, exceeding current material capabilities. Energy harvesting technologies open new avenues for devices to operate self-powered, eliminating the need for traditional energy storage methods. Utilizing mechanical movements, thermal, solar energy, and moisture gradients holds promise, yet achieving a consistent and reliable energy source requires further development. Integrating these harvesting technologies with advanced energy storage could offer a solution. Advances in material science, physics, and chemistry are crucial for miniaturizing devices and enhancing performance, ensuring they are safe and biocompatible.

6.1. Energy Harvesting Efficiency

Commercial implantable medical devices such as neural stimulators require high operation frequency and high power. Moreover, the energy harvesters inside the human body mainly rely on mechanical energy from low-frequency motion of human internal organs. It is still challenging for current nanogenerators to provide continuous power to commercial medical devices. TENGs and PENGs for implantable medical devices, such as cardiac pacemakers and neural stimulators, currently produce power densities from 0.001 to 0.1 mW cm⁻² as seen in **Figures 7** and **11**. Bridging the gap between these power levels and the requirements of commercial medical devices (**Figure 7**) is crucial for future advancements. Based on device weight, the gravimetric peak power of twistron mechanical energy harvesters substantially exceeds those of any other mechanical energy harvesters for a deformation frequency range between 0.01 and 120 Hz.^[94] While many sensing applications operate within this power range, energy needs for stimulation beyond cardiac pacing are significantly higher, highlighting the need for innovative design improvements in power harvesting.

There are a few aspects could considerably improve the output of energy harvesters. Using TENG as an example, for it to meet the requirements for large-scale commercial applications, they need to produce high power output. High surface charge density leads to high energy output. However, the surface charge density of TENG are influenced by triboelectrification charge density, air breakdown, and dielectric breakdown. Numerous effects have been focused on improving the performance of TENG by increasing triboelectric charge density. Optimization of materials

and structural designs is frequently involved in this. For example, thinner dielectric film, larger dielectric constant, and lower atmospheric pressure always lead to a higher maximum surface charge density.^[192] These enhancements have a direct effect on energy conversion efficiency, which then improves the energy output. Surface modification,^[193] ion injection,^[65] and charge-excitation^[194] are widely used for improving triboelectric charge density. However, it is equally important to address the issue of triboelectric charge decay caused by air breakdown, which is an area often neglected in past studies. Reducing triboelectric charge decay can substantially improve TENG performance. Therefore, more research should focus on understanding the fundamental mechanisms of triboelectric charge decay and developing advanced strategies to minimize it.

Furthermore, TENGs present several challenges in practical applications, particularly due to environmental factors. Specifically, high relative humidity conditions may significantly degrade the power outputs of TENGs. The presence of atmospheric moisture, absorbed on the surface of the TENGs' triboelectric layers, facilitates the transportation and dissipation of triboelectric charges.^[195,196] This phenomenon severely diminishes both the output performance and stability of TENGs, which limits their practical utility. Addressing the degradation of TENG performance in humid environments is crucial, as humidity is commonly encountered in many practical settings where TENGs are deployed.

To mitigate these effects, various approaches have been developed, including the use of superhydrophobic materials in the triboelectric layers and encapsulation of the devices to shield them from moisture.^[197–199] These modifications aim to enhance the humidity resistance of TENGs. Despite these improvements, the output levels of many TENGs remain insufficient for many practical applications. Therefore, advancing the mechanical robustness and triboelectric properties of TENGs under conditions of high relative humidity is essential to expand their practical applications and ensure their reliable operation in typical environmental conditions.

Another strategy to increase energy harvesting efficiency is to reduce system energy loss that can arise from resistance mismatches or heat dissipation when the harvested energy is used to charge energy storage devices. Most energy harvesters output a low voltage insufficient to directly power medical devices or charge energy storage devices. Hence, voltage amplifiers are needed in most cases boosts the voltage. The efficiency of the amplifiers or power management units is then also an important consideration for avoiding significant energy losses.

6.2. Long-Term Biocompatibility and Safety

Wearable and implantable energy harvesters require long-term biocompatibility and safety. For devices intended to be implanted, these criteria are particularly critical to prevent adverse reactions within the body. Implantable energy harvesters are engineered to maintain long-term and direct contact with internal body tissues and fluids. Consequently, it is essential to ensure that the materials utilized in these implantable devices are biocompatible to prevent inflammatory responses and potential risk of toxicity. The selection and innovation of these nontoxic materials face a

Table 4. Comparison among different energy harvesters, wireless energy transfer devices, and energy storage devices.

Technologies	Method	Advantages	Limitations
Energy harvesting technologies	Triboelectric nanogenerator (TENG)	High power density, output voltage and efficiency Extensive variety of material choices	Low output current due to high output impedance The lifespan is constrained due to unavoidable wear and friction between layers
	Piezoelectric nanogenerator (PENG)	Micro- and nanoscale fabrication High energy density	Output performance affected by ambient humidity Potential concerns regarding the biological compatibility of ceramics containing lead
	Electromagnetic energy harvester (EMEH)	Micro- and nanoscale fabrication High efficiency and output current High power density	Expensive materials Low efficiency at low frequency operation Low output voltage
	Thermoelectric energy generator (TEG)	Robust Continuous DC output Robust and long operational lifetime	Frequency dependent output Highly depending on temperature difference Low energy conversion efficiency
Wireless energy transfer technologies	Photovoltaic (PV) energy harvester	Independent from frequency Inexhaustible and abundant energy source Continuous DC output Mature technology	Restrict placement site for implantation Highly depend on irradiance humidity Reduce of output power with increasing tissue thickness Implant depth is limited by reduced output with increasing tissue thickness
	Moisture-driven energy generator (MEG)	Independent from wide range of environments	Low energy density Short-term electricity generation
	Inductive power transfer Capacitive power transfer Radio frequency power transfer Ultrasound power transfer	High output power High output power Facilitate both signal transmission and power transfer High efficiency High power density	Potential heating issues Large size Influenced by environmental factors Low output power Limited lifespan Large size Limited lifespan
Energy storage	Battery Supercapacitor	Fast rate of charging and discharging	Low energy density

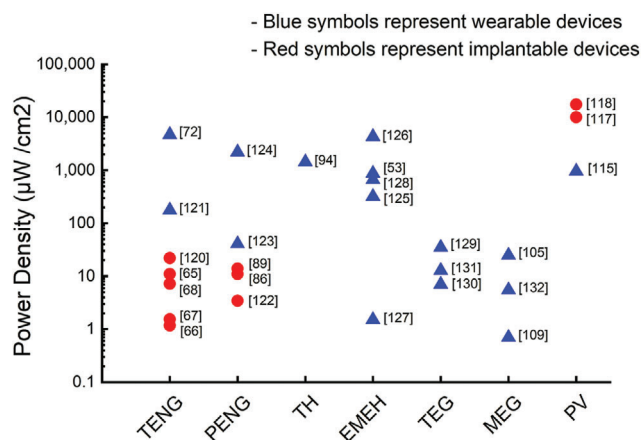


Figure 11. Power density comparison for different energy harvesting technologies. Each symbol represents the peak power density in publications from 2018 to 2024. Different energy harvesting technologies include: TENG,^[65–68,72,120,121] PENG,^[86,89,122–124] twistron harvester (TH),^[94] electromagnet generator (EMEH),^[53,125–128] thermoelectric generator (TEG),^[129–131] and moisture-driven energy generator (MEG).^[105,109,132] Photovoltaic energy harvester (PV) under 1000 W m⁻² solar irradiation.^[115,117,118]

substantial challenge. Biocompatibility cannot be solely assessed based on the toxicity of materials, as it can be influenced by any process or contamination like inaccurate material mixing or tool contamination.

Surprisingly, many studies have not paid much attention to evaluating the final product's biocompatibility, relying solely on the biocompatibility of the constituent materials, potentially leading to erroneous performance assessments. Furthermore, ensuring the long-term stability of these materials inside the human body is critically important because any degradation can potentially affect both performance and safety of the energy harvesting devices. Therefore, more studies are needed to assess the long-term performance and safety of implants.

Furthermore, it is necessary for implantable energy harvesting devices to achieve mechanical compatibility with adjacent tissues to prevent discomfort or harm. Additionally, given that many energy harvesters operate based on electrical principles, electrical safety cannot be ignored. Potential risks such as electrical shorts need to be effectively managed. By ensuring proper isolation and protection against electrical errors, the safety profile of these devices can be significantly enhanced.

The rapid growth of wearable and portable electronic devices has led to a significant increase in material waste and discarded electronic components, posing a considerable environmental challenge. The ideal scenario is to develop electronic devices that can be either recycled or biodegraded after their useful life. At present, the primary materials used in wearable energy harvesters, such as TENGs and PENGs, are primarily polymers and metals.^[82,200] These materials are chosen for their excellent electrical output and triboelectric properties. However, they are not readily recyclable or biodegradable, contributing to resource depletion and environmental pollution due to their extensive use.

Consequently, the focus on developing renewable, biocompatible, and environmentally degradable materials like cellulose, chitosan, gelatin, and starch is emerging as a major research

direction.^[201–205] These materials are viewed as viable alternatives that could mitigate the environmental impacts of traditional non-degradable materials. Moreover, reusing eco-friendly waste materials not only addresses environmental concerns but also offers a solution to the looming energy crisis by providing sustainable materials for energy harvesting applications.

6.3. Device Functionality

DC output: Overall, most electronic devices require constant DC voltage. Most energy harvesters based on PENGs and TENGs, however, produce AC outputs. There are several drawbacks of AC outputs. First, rectifiers must be used to transfer AC to DC to allow the electricity to be stored in rechargeable batteries and supercapacitors. Therefore, the overall energy efficiency will be decreased since the rectifier will consume $\approx 10\text{--}15\%$ of the harvested energy. Also, rigid rectifiers also add weight and bulk to medical devices. Another issue with AC output is that it will cause energy output instability which will seriously influence its performance in energy storage and electronic powering.^[206] Therefore, DC output energy harvesters are more desirable because they can directly power electronic devices and recharge energy storage units. Up to now, strategies such as continuous electrostatic breakdown,^[206] periodical lateral cantilevers,^[207] and multiphase rotation-type structures^[208] have been employed to generate DC output. However, none of these methods can be applied to implantable devices. Thus, directly generating DC outputs for WIMDs is still an open challenge.

Controllable output: Most recent research has focused on using the electricity produced by PENGs and TENGs from the motions of internal organs to stimulate nerve system. One issue with this approach is the lack of control over the electric pulses, which are typically of low frequency due to the energy harvesting from internal organs that move at relatively low frequency. However, the neural stimulator or cardiac pacemaker needs some stimulations at specific frequencies, pulse width, and current threshold depending on different patients' needs in real clinical applications. Currently, it is not possible to generate controllable outputs from energy harvesters that can be used directly in nerve stimulators without an external power source. By contrast, wireless energy transfer technologies such as ultrasound-induced energy harvesters can transit sufficient energy into the human body, but the power source of the ultrasound transmitter makes this approach inconvenient.

With the goal of minimizing the potential impact and discomfort experienced by patients, it is crucial to keep implantable devices as lightweight and small as possible. Currently, most of the energy harvesters have a relative low power density, thus requiring a large size to achieve the power demanded by WIMDs. Advanced in this enhancing the energy harvesting density of these devices will bring significant benefits.

6.4. Hybrid Energy Harvesting Devices

There are various types of energy harvesting technologies, including TENGs, PENGs, twistron harvesters, electromagnetic generators, thermoelectric generators, moisture-driven energy

generators, and photovoltaic energy harvesters. These technologies capture sustainable energy from diverse sources including kinetic motion, solar radiation, atmospheric humidity, wind, and heat. Although each system is efficient at converting a specific type of green energy, its performance is significantly impacted by the environmental conditions. For instance, biomechanical energy harvesters can generate energy both indoors and outdoors but require biomechanical movement at specific locations. When users are stationary, no energy is harvested.^[209] Similarly, photovoltaic energy harvesters are effective under direct sunlight, but their performance is limited by changing weather conditions.^[113,115] Therefore, it is critical to develop continuous energy harvesting systems to ensure uninterrupted power supply for medical devices.

Natural and artificial energy sources, such as light, solar, heat, wind, heartbeats, and humidity are consistently available. Therefore, integrating mechanical, photovoltaic, moisture-driven and thermal energy harvesting systems has the potential to provide continuous energy generation. For example, during the day, solar energy can serve as the primary energy source for hybrid energy harvesting devices, supplemented by mechanical and thermal energy sources to enhance the output. Conversely, under night-time or rainy conditions, mechanical or thermal energy harvesting systems outperform photovoltaic energy harvesting systems. Thus, hybrid energy harvesters can effectively capture energy, providing a continuous and reliable power source for medical devices.

However, it remains a major challenge to design and build hybrid systems so that they can work collaboratively as a system, because each of the energy harvesting mechanisms will require its own materials and designs, making it difficult to integrate them together without degrading their individual performance. In addition, hybrid devices may also require complex circuit and power management systems, which must also be sufficiently miniaturized to fit within the implantable devices.^[210-212] Therefore, it is essential to design hybrid systems where the different elements are synergistic, thus reducing wiring and integration challenges. For example, combining triboelectric or piezoelectric energy harvesters with wireless power transfer technology is a promising approach to harvesting energy from external sources. Overall, hybrid energy harvesters have the potential to achieve higher energy output, but significant challenges in system integration and safety need to be addressed to realize their full potential.

6.5. Standardization

Substantial progress has been made at the laboratory level in developing high-performance energy harvesters. Moving forward, it will be essential to focus on developing techniques to improve the long-term effectiveness and durability, as well as cost-effectiveness to accelerate the commercialization of these energy harvesters.

There is an urgent need to establish a comprehensive framework for measuring and comparing the outputs and efficiencies of energy harvesters. Currently, metrics such as open-circuit voltage (V_{oc}), short-circuit current (I_{sc}), and power density are used for comparison. However, these parameters can vary significantly depending on the test conditions, such as frequency and applied forces, which can particularly affect the performance of TENGs

and PENGs. Variations in humidity levels also influence the results. Inconsistencies in reporting these parameters alongside different testing conditions pose significant challenges to the design and sizing of energy harvesters to meet the specific energy needs of WIMDs.

Differences in the units of measurement reported in the literature further complicate the comparison of the energy harvesters' performance characteristics. Establishing standardized testing protocols is vital for advancing the field and facilitating the commercial scalability and consistent evaluation of energy harvesting technologies.

In summary, the successful implementation of energy harvesters in practical applications requires not only advancements in material preparation and device engineering but also the establishment of robust standards and protocols. These standards will ensure consistency in data and transferability among different devices, which is crucial for the integration of diverse systems and the advancement of collaborative technologies in the field of bioelectronics.

7. Conclusion

Remarkable advancements have been made in the development of energy harvesters, wireless charging, and flexible energy storage units for powering wearable and implantable active medical devices. Currently, most WIMDs depend heavily on large, short-lived primary batteries that require frequent replacement, leading to poor experiences for patients. However, novel developments in energy harvesting technologies, including mechanical energy harvesters like triboelectric, piezoelectric nanogenerators, and carbon nanotube yarn nanogenerators known as twistron harvesters, along with electromagnetic generators, are being designed to harness energy from mechanical movements both outside and inside the human body. Moreover, thermoelectric generators have shown some promise in generating electrical energy from waste body heat, while moisture-driven energy harvesters are emerging as a novel technology to harness energy from environmental humidity gradients. While these pioneering technologies are still in their infancy and have not been widely adopted for clinical applications, they represent significant potential for revolutionizing future active medical devices. Beyond the scope of energy harvesting, wireless energy transmission technologies, including inductive, capacitive, RF, and ultrasound, are emerging to achieve self-powered WIMDs.

Despite the considerable progress made, substantial obstacles persist in the development of energy solutions for WIMDs. This review has identified several critical gaps and promising pathways for further research. These include increasing energy harvesting efficiencies; meeting the power needs of high-energy-demand devices such as neural stimulators; ensuring long-term biocompatibility and safety for devices intended for implantation; and improving device functionality through adjustable stimulation frequencies. Moreover, there is a pressing need for energy harvesters to provide DC output to directly power WIMDs and/or recharge energy storage devices, as most current harvesters produce AC outputs. Furthermore, reducing the size of implantable energy harvesters is essential to minimize patient discomfort while maintaining high power output, which necessitates advances in materials science and micromanufacturing

techniques. Additionally, hybrid energy harvesters that combine different mechanisms to harness diverse energy sources could capture significantly more energy than single-mechanism systems. Beyond technological advancements, the successful deployment of energy harvesters in practical settings also requires the development of robust standards and protocols. Establishing these standards is crucial for ensuring data consistency and facilitating synergy among different devices, which is essential for the integration of diverse systems and fostering collaborative advancements in the field of bioelectronics.

While significant challenges remain in fully realizing self-powered WIMDs, recent advancements in advanced materials and devices have brought that goal within exciting reach. By tackling the challenges outlined in this review, a future where wearable and implantable medical devices can be entirely powered by the human body or the energy in the surrounding environment is increasingly feasible.

Acknowledgements

Z.G. and Y.Z. contributed equally to this work. Z.G., J.Z., S.P., and C.H.W. would like to thank the financial support from the Australian Research Council under the Industry Transformation Research Hub (IH210100040). J.Z. acknowledges the support from the Australian Research Council on her future fellowship (FT230100116).

Open access publishing facilitated by University of New South Wales, as part of the Wiley - University of New South Wales agreement via the Council of Australian University Librarians.

Conflict of Interest

The authors declare no conflict of interest.

Keywords

active medical devices, energy harvesters, energy storage, wireless power transfer

Received: March 27, 2024

Revised: June 21, 2024

Published online:

- [1] Y. Gai, Y. Jiang, Z. Li, *Nano Energy* **2023**, *116*, 108787.
- [2] Y. Khan, A. E. Ostfeld, C. M. Lochner, A. Pierre, A. C. Arias, *Adv. Mater.* **2016**, *28*, 4373.
- [3] S. M. A. Iqbal, I. Mahgoub, E. Du, M. A. Leavitt, W. Asghar, *npj Flexible Electron.* **2021**, *5*, 9.
- [4] F. P. Pons-Faudoa, A. Ballerini, J. Sakamoto, A. Grattoni, *Biomed. Microdevices* **2019**, *21*, 47.
- [5] S. Wang, Q. Cui, P. Abiri, M. Roustaei, E. Zhu, Y.-R. Li, K. Wang, S. Duarte, L. Yang, R. Ebrahimi, M. Bersohn, J. Chen, T. K. Hsiai, *Sci. Adv.* **2023**, *9*, eadj0540.
- [6] J. Zhang, R. Das, J. Zhao, N. Mirzai, J. Mercer, H. Heidari, *Adv. Mater. Technol.* **2022**, *7*, 2101086.
- [7] P. Li, G.-H. Lee, S. Y. Kim, S. Y. Kwon, H.-R. Kim, S. Park, *ACS Nano* **2021**, *15*, 1960.
- [8] T. Loncar-Turukalo, E. Zdravetski, J. M. da Silva, I. Chouvarda, V. Trajkovic, *J. Med. Internet Res.* **2019**, *21*, 14017.

- [9] Y. J. Hong, H. Jeong, K. W. Cho, N. Lu, D.-H. Kim, *Adv. Funct. Mater.* **2019**, *29*, 1808247.
- [10] C. Shi, Z. Tang, H. Zhang, Y. Liu, *IEEE Trans. Instrum. Meas.* **2023**, *72*, 1.
- [11] Straits Research team, Active Implantable Medical Devices Market, [https://straitsresearch.com/report/active-implantable-medical-devices-market#:~:text=Market%20Overview,period%20\(2023%E2%80%932031\)](https://straitsresearch.com/report/active-implantable-medical-devices-market#:~:text=Market%20Overview,period%20(2023%E2%80%932031)) (accessed: March 2024).
- [12] V. Nair, A. N. Dalrymple, Z. Yu, G. Balakrishnan, C. J. Bettinger, D. J. Weber, K. Yang, J. T. Robinson, *Science* **2023**, *382*, 4732.
- [13] C. Ning, R. Cheng, Y. Jiang, F. Sheng, J. Yi, S. Shen, Y. Zhang, X. Peng, K. Dong, Z. L. Wang, *ACS Nano* **2022**, *16*, 2811.
- [14] Z. L. Wang, J. Song, *Science* **2006**, *312*, 242.
- [15] A. Wang, Z. Liu, M. Hu, C. Wang, X. Zhang, B. Shi, Y. Fan, Y. Cui, Z. Li, K. Ren, *Nano Energy* **2018**, *43*, 63.
- [16] S. H. Kim, C. S. Haines, N. Li, K. J. Kim, T. J. Mun, C. Choi, J. Di, Y. J. Oh, J. P. Oviedo, J. Bykova, S. Fang, N. Jiang, Z. Liu, R. Wang, P. Kumar, R. Qiao, S. Priya, K. Cho, M. Kim, M. S. Lucas, L. F. Drummy, B. Maruyama, D. Y. Lee, X. Lepró, E. Gao, D. Albarq, R. Ovalle-Robles, S. J. Kim, R. H. Baughman, *Science* **2017**, *357*, 773.
- [17] C. Moerke, A. Wolff, H. Ince, J. Ortak, A. Öner, *Herzschrittmachertherapie Elektrophysiologie* **2022**, *33*, 224.
- [18] D. M. Moore, C. McCrory, *BJA Educ.* **2016**, *16*, 258.
- [19] R. Ramasubbu, S. Lang, Z. H. T. Kiss, *Front. Psychiatry* **2018**, *9*, 302.
- [20] E. Musk, *J. Med. Internet Res.* **2019**, *21*, 16194.
- [21] B. Yan, D. An, X. Wang, B. J. DeLong, A. Kiourti, K. Dungan, J. L. Volakis, M. Ma, L. Guo, *Med. Devices Sens.* **2019**, *2*, 10055.
- [22] S.-Y. Yang, V. Sencadas, S. S. You, N. Z.-X. Jia, S. S. Srinivasan, H.-W. Huang, A. E. Ahmed, J. Y. Liang, G. Traverso, *Adv. Funct. Mater.* **2021**, *31*, 2009289.
- [23] H. A. Yiğit, H. Uluşan, M. B. Yuksel, S. Chamanian, B. Çiftci, A. Koyuncuoğlu, A. Muhtaroglu, H. Külah, in *2019 IEEE/ACM Int. Symp. on Low Power Electronics and Design (ISLPED)*, Lausanne, Switzerland, **2019**, pp. 1–5.
- [24] Z. Wang, S. Mai, C. Zhang, in *4th IEEE Int. Symp. on Electronic Design, Test and Applications, Delta 2008*, Hong Kong, China, **2008**, pp. 163–166.
- [25] D. Accoto, M. Calvano, D. Campolo, F. Salvinelli, E. Guglielmelli, in *2009 Annual Int. Conf. of the IEEE Engineering in Medicine and Biology Society*, Minneapolis, MN, USA, **2009**, pp. 4860–4863.
- [26] J. Dieffenderfer, H. Goodell, S. Mills, M. McKnight, S. Yao, F. Lin, E. Beppler, B. Bent, B. Lee, V. Misra, Y. Zhu, O. Oralkan, J. Strohmaier, J. Muth, D. Peden, A. Bozkurt, *IEEE J. Biomed. Health Inf* **2016**, *20*, 1251.
- [27] T. Salo, K.-U. Kirstein, J. Sedivy, J. Grunenfelder, T. Vancura, G. Zund, H. Baltés, in *26th Annual Int. Conf. of the IEEE Engineering in Medicine and Biology Society* San Francisco, CA, USA, **2004**, pp. 23226–23229.
- [28] H. Lee, E. Kim, Y. Lee, H. Kim, J. Lee, M. Kim, H.-J. Yoo, S. Yoo, *Sci. Adv.* **2018**, *4*, 9530.
- [29] B. Larsson, H. Elmqvist, L. Rydén, H. Schüller, *Pacing Clin. Electrophysiol.* **2003**, *26*, 114.
- [30] V. Parsonnet, J. Driller, D. Cook, S. A. Rizvi, *Pacing Clin. Electrophysiol.* **2006**, *29*, 195.
- [31] K. Jeffrey, V. Parsonnet, *Circulation* **1998**, *97*, 1978.
- [32] T. E. Schlaepfer, B. H. Bewernick, S. Kayser, B. Mädler, V. A. Coenen, *Biol. Psychiatry* **2013**, *73*, 1204.
- [33] M. Kronenbuerger, S. Zobel, J. Ilgner, A. Finkelmeyer, P. Reinacher, V. A. Coenen, H. Wilms, M. Kloss, K. Kiening, C. Daniels, D. Falk, J. B. Schulz, G. Deuschl, T. Hummel, *Exp. Neurol.* **2010**, *222*, 144.
- [34] T. C. Zhang, J. J. Janik, W. M. Grill, *Brain Res.* **2014**, *1569*, 19.
- [35] P. S. Larson, *Neurotherapeutics* **2014**, *11*, 465.
- [36] G. Gu, N. Zhang, C. Chen, H. Xu, X. Zhu, *ACS Nano* **2023**, *17*, 9661.
- [37] S. L. Metzger, K. T. Littlejohn, A. B. Silva, D. A. Moses, M. P. Seaton, R. Wang, M. E. Dougherty, J. R. Liu, P. Wu, M. A. Berger,

- I. Zhuravleva, A. Tu-Chan, K. Ganguly, G. K. Anumanchipalli, E. F. Chang, *Nature* **2023**, 620, 1037.
- [38] F. R. Willett, E. M. Kunz, C. Fan, D. T. Avansino, G. H. Wilson, E. Y. Choi, F. Kamdar, M. F. Glasser, L. R. Hochberg, S. Druckmann, K. V. Shenoy, J. M. Henderson, *Nature* **2023**, 620, 1031.
- [39] G. Hong, C. M. Lieber, *Nat. Rev. Neurosci.* **2019**, 20, 330.
- [40] T. Murata, S. Nirengi, N. Sakane, A. Kuroda, Y. Hirota, M. Matsuhisa, M. Namba, T. Kobayashi, *J. Diabetes Invest.* **2018**, 9, 903.
- [41] F.-G. Zeng, S. Rebscher, W. Harrison, X. Sun, H. Feng, *IEEE Rev. Biomed. Eng.* **2008**, 1, 115.
- [42] D. Chaudhuri, S. Kundu, N. Chattoraj, in *2017 Innovations in Power and Advanced Computing Technologies (i-PACT)*, **2017**, pp. 1–5.
- [43] Visionflex, VF Fingertip Pulse Oximeter, <https://www.visionflex.com/product/peripherals/pulse-oximeters/vf-fingertip-pulse-oximeter/> (accessed: March 2024).
- [44] Y. Gai, E. Wang, M. Liu, L. Xie, Y. Bai, Y. Yang, J. Xue, X. Qu, Y. Xi, L. Li, D. Luo, Z. Li, *Small Methods* **2022**, 6, 2200653.
- [45] Y. Feng, X. Huang, S. Liu, W. Guo, Y. Li, H. Wu, *Nano Energy* **2019**, 62, 197.
- [46] Z. Li, Q. Zheng, Z. L. Wang, Z. Li, *Research* **2020**, 2020, 25.
- [47] M. Alhawari, B. Mohammad, H. Saleh, M. Ismail, *Springer International Publishing* **2018**, 4, 5.
- [48] H. Ouyang, J. Tian, G. Sun, Y. Zou, Z. Liu, H. Li, L. Zhao, B. Shi, Y. Fan, Y. Fan, Z. L. Wang, Z. Li, *Adv. Mater.* **2017**, 29, 1703456.
- [49] X. Zhang, Z. Zhang, Y. Li, C. Liu, Y. X. Guo, Y. Lian, in *2015 IEEE Asian Solid-State Circuits Conf. - SSSCC*, Xiamen, China, **2015**, pp. 1–4.
- [50] A. Roy, A. Klinefelter, F. B. Yahya, X. Chen, L. P. Gonzalez-Guerrero, C. J. Lukas, D. A. Kamakshi, J. Boley, K. Craig, M. Faisal, S. Oh, N. E. Roberts, Y. Shakhsher, A. Shrivastava, D. P. Vasudevan, D. D. Wentzloff, B. H. Calhoun, *IEEE Trans. Biomed. Circuits Syst.* **2015**, 9, 862.
- [51] T. Starner, *IBM Syst. J.* **1996**, 35, 618.
- [52] R. Khusainov, D. Azzi, I. E. Achumba, S. D. Bersch, *Sensors* **2013**, 13, 12852.
- [53] P. Maharjan, T. Bhatta, M. Salauddin Rasel, Md. Salauddin, M. Toyabur Rahman, J. Y. Park, *Appl. Energy* **2019**, 256, 113987.
- [54] C. Xu, Y. Song, M. Han, H. Zhang, *Microsyst. Nanoeng.* **2021**, 7, 25.
- [55] F.-R. Fan, Z.-Q. Tian, Z. L. Wang, *Nano Energy* **2012**, 1, 328.
- [56] Z. L. Wang, in *Handbook of Triboelectric Nanogenerators* (Eds: Z. L. Wang, Y. Yang, J. Zhai, J. Wang), Springer International Publishing, Cham **2023**, pp. 3–32.
- [57] H. Wang, J. Yang, S. Umer, N. Zhu, G. Yang, Y. Li, J. Yan, *Polym. Compos.* **2024**, 45, 1208.
- [58] X. Chen, Y. Liu, Y. Sun, T. Zhao, C. Zhao, T. A. Khattab, E. G. Lim, X. Sun, Z. Wen, *Nano Energy* **2022**, 98, 107236.
- [59] I. Aazem, D. Treasa Mathew, S. Radhakrishnan, K. V. Vijoy, H. John, D. M. Mulvihill, S. C. Pillai, *RSC Adv.* **2022**, 12, 10545.
- [60] G. Li, J. Zhang, F. Huang, S. Wu, C.-H. Wang, S. Peng, *Nano Energy* **2021**, 88, 106289.
- [61] K. Parida, G. Thangavel, G. Cai, X. Zhou, S. Park, J. Xiong, P. S. Lee, *Nat. Commun.* **2019**, 10, 2158.
- [62] I. Aazem, D. T. Mathew, S. Radhakrishnan, K. V. Vijoy, H. John, D. M. Mulvihill, S. C. Pillai, *RSC Adv.* **2022**, 12, 10545.
- [63] W.-T. Cao, H. Ouyang, W. Xin, S. Chao, C. Ma, Z. Li, F. Chen, M.-G. Ma, *Adv. Funct. Mater.* **2020**, 30, 2004181.
- [64] X. Pu, M. Liu, X. Chen, J. Sun, C. Du, Y. Zhang, J. Zhai, W. Hu, Z. L. Wang, *Sci. Adv.* **2017**, 3, 1700015.
- [65] H. Ouyang, Z. Liu, N. Li, B. Shi, Y. Zou, F. Xie, Y. Ma, Z. Li, H. Li, Q. Zheng, X. Qu, Y. Fan, Z. L. Wang, H. Zhang, Z. Li, *Nat. Commun.* **2019**, 10, 1821.
- [66] H. Ryu, H. Park, M.-K. Kim, B. Kim, H. S. Myoung, T. Y. Kim, H.-J. Yoon, S. S. Kwak, J. Kim, T. H. Hwang, E.-K. Choi, S.-W. Kim, *Nat. Commun.* **2021**, 12, 4374.
- [67] Z. Liu, Y. Hu, X. Qu, Y. Liu, S. Cheng, Z. Zhang, Y. Shan, R. Luo, S. Weng, H. Li, H. Niu, M. Gu, Y. Yao, B. Shi, N. Wang, W. Hua, Z. Li, Z. L. Wang, *Nat. Commun.* **2024**, 15, 507.
- [68] F. Jin, T. Li, T. Yuan, L. Du, C. Lai, Q. Wu, Y. Zhao, F. Sun, L. Gu, T. Wang, Z.-Q. Feng, *Adv. Mater.* **2021**, 33, 2104175.
- [69] W. Li, Z. Song, H. Kong, M. Chen, S. Liu, Y. Bao, Y. Ma, Z. Sun, Z. Liu, W. Wang, L. Niu, *Nano Energy* **2022**, 104, 107935.
- [70] T. He, Q. Shi, H. Wang, F. Wen, T. Chen, J. Ouyang, C. Lee, *Nano Energy* **2019**, 57, 338.
- [71] J. Zhang, H. Wang, P. Blanloeuil, G. Li, Z. Sha, D. Wang, W. Lei, C. Boyer, Y. Yu, R. Tian, C. H. Wang, *Compos. Commun.* **2020**, 22, 100535.
- [72] Y. He, H. Wang, Z. Sha, C. Boyer, C.-H. Wang, J. Zhang, *Nano Energy* **2022**, 98, 107343.
- [73] Z. Sha, C. Boyer, G. Li, Y. Yu, F.-M. Allieux, K. Kalantar-Zadeh, C.-H. Wang, J. Zhang, *Nano Energy* **2022**, 92, 106713.
- [74] F. Ali, W. Raza, X. Li, H. Gul, K.-H. Kim, *Nano Energy* **2019**, 57, 879.
- [75] H. Li, C. Tian, Z. D. Deng, *Appl. Phys. Rev.* **2014**, 1, 041301.
- [76] S. Mirjalali, R. Bagherzadeh, A. Mahdavi Varposhti, M. Asadnia, S. Huang, W. Chang, S. Peng, C.-H. Wang, S. Wu, *ACS Appl. Mater. Interfaces* **2023**, 15, 41806.
- [77] S. Mirjalali, R. Bagherzadeh, S. Abrishami, M. Asadnia, S. Huang, A. Michael, S. Peng, C.-H. Wang, S. Wu, *Macromol. Mater. Eng.* **2023**, 308, 2300009.
- [78] M. S. Sorayani Bafqi, R. Bagherzadeh, M. Latifi, *J. Polym. Res.* **2015**, 22, 130.
- [79] S. Mohammadpourfazeli, S. Arash, A. Ansari, S. Yang, K. Mallick, R. Bagherzadeh, *RSC Adv.* **2023**, 13, 370.
- [80] P. Fakhri, N. Eaianli, R. Bagherzadeh, B. Jaleh, M. Kashfi, R. Fausto, *Sci. Rep.* **2023**, 13, 16412.
- [81] B. H. Moghadam, M. Hasanzadeh, A. Simchi, *ACS Appl. Nano Mater.* **2020**, 3, 8742.
- [82] P. Maiti, A. Sasmal, A. Arockiarajan, R. Mitra, *Sustainable Energy Fuels* **2024**, 8, 729.
- [83] S. D. Mahapatra, P. C. Mahapatra, A. I. Aria, G. Christie, Y. K. Mishra, S. Hofmann, V. K. Thakur, *Adv. Sci.* **2021**, 8, 2100864.
- [84] K.-Y. Shin, J. S. Lee, J. Jang, *Nano Energy* **2016**, 22, 95.
- [85] J. Park, R. Ghosh, M. S. Song, Y. Hwang, Y. Tchoe, R. K. Saroj, A. Ali, P. Guha, B. Kim, S.-W. Kim, M. Kim, G.-C. Yi, *NPG Asia Mater.* **2022**, 14, 40.
- [86] N. Li, Z. Yi, Y. Ma, F. Xie, Y. Huang, Y. Tian, X. Dong, Y. Liu, X. Shao, Y. Li, L. Jin, J. Liu, Z. Xu, B. Yang, H. Zhang, *ACS Nano* **2019**, 13, 2822.
- [87] M. Novák, J. Rosina, H. Bendová, K. Kejlová, A. Vlková, M. Rucki, L. Svobodová, R. Gürlich, J. Hajer, *Sci. Rep.* **2023**, 13, 1644.
- [88] P. Thainirarnit, P. Yingyong, D. Isarakorn, *Sensors* **2020**, 20, 5828.
- [89] S. Azimi, A. Golabchi, A. Nekookar, S. Rabbani, M. H. Amiri, K. Asadi, M. M. Abolhasani, *Nano Energy* **2021**, 83, 105781.
- [90] Q. Zheng, H. Zhang, B. Shi, X. Xue, Z. Liu, Y. Jin, Y. Ma, Y. Zou, X. Wang, Z. An, W. Tang, W. Zhang, F. Yang, Y. Liu, X. Lang, Z. Xu, Z. Li, Z. L. Wang, *ACS Nano* **2016**, 10, 6510.
- [91] J. Li, T. A. Hacker, H. Wei, Y. Long, F. Yang, D. Ni, A. Rodgers, W. Cai, X. Wang, *Nano Energy* **2021**, 90, 106507.
- [92] M. Han, H. Wang, Y. Yang, C. Liang, W. Bai, Z. Yan, H. Li, Y. Xue, X. Wang, B. Akar, H. Zhao, H. Luan, J. Lim, I. Kandela, G. A. Ameer, Y. Zhang, Y. Huang, J. A. Rogers, *Nat. Electron.* **2019**, 2, 26.
- [93] D. Y. Park, D. J. Joe, D. H. Kim, H. Park, J. H. Han, C. K. Jeong, H. Park, J. G. Park, B. Joung, K. J. Lee, *Adv. Mater.* **2017**, 29, 1702308.
- [94] M. Zhang, W. Cai, Z. Wang, S. Fang, R. Zhang, H. Lu, A. E. Aliev, A. A. Zakhidov, C. Huynh, E. Gao, J. Oh, J. H. Moon, J. W. Park, S. J. Kim, R. H. Baughman, *Nat. Energy* **2023**, 8, 203.
- [95] Y. Jang, S. M. Kim, K. J. Kim, H. J. Sim, B.-J. Kim, J. W. Park, R. H. Baughman, A. Ruhparwar, S. J. Kim, *ACS Sens.* **2019**, 4, 2893.

- [96] A. Ruhparwar, A. Osswald, H. Kim, R. Wakili, J. Müller, N. Pizanis, F. Al-Rashid, U. Hendgen-Cotta, T. Rassaf, S. J. Kim, *Adv. Mater.* **2024**, 2313688.
- [97] J. R. Busch, S. H. Hansen, *Forensic Sci. Int.* **2022**, 335, 111283.
- [98] A. Zurbuchen, A. Haeberlin, L. Bereuter, J. Wagner, A. Pfenniger, S. Omari, J. Schaerer, F. Jutzi, C. Huber, J. Fuhrer, R. Vogel, *Heart Rhythms* **2017**, 14, 294.
- [99] A. Zurbuchen, A. Haeberlin, A. Pfenniger, L. Bereuter, J. Schaerer, F. Jutzi, C. Huber, J. Fuhrer, R. Vogel, *IEEE Trans. Biomed. Circuits Syst.* **2017**, 11, 78.
- [100] C. S. Kim, G. S. Lee, H. Choi, Y. J. Kim, H. M. Yang, S. H. Lim, S.-G. Lee, B. J. Cho, *Appl. Energy* **2018**, 214, 131.
- [101] D. Singh, A. Choudhary, A. Garg, *ACS Appl. Mater. Interfaces* **2018**, 10, 2793.
- [102] R. Feng, F. Tang, N. Zhang, X. Wang, *ACS Appl. Mater. Interfaces* **2019**, 11, 38616.
- [103] M. Hyland, H. Hunter, J. Liu, E. Veety, D. Vashae, *Appl. Energy* **2016**, 182, 518.
- [104] L. Li, Z. Chen, M. Hao, S. Wang, F. Sun, Z. Zhao, T. Zhang, *Nano Lett.* **2019**, 19, 5544.
- [105] K. Zhao, J. W. Lee, Z. G. Yu, W. Jiang, J. W. Oh, G. Kim, H. Han, Y. Kim, K. Lee, S. Lee, H. Kim, T. Kim, C. E. Lee, H. Lee, J. Jang, J. W. Park, Y.-W. Zhang, C. Park, *ACS Nano* **2023**, 17, 5472.
- [106] G. Xue, Y. Xu, T. Ding, J. Li, J. Yin, W. Fei, Y. Cao, J. Yu, L. Yuan, L. Gong, J. Chen, S. Deng, J. Zhou, W. Guo, *Nat. Nanotechnol.* **2017**, 12, 317.
- [107] S. Lin, X. Chen, Z. L. Wang, *Chem. Rev.* **2022**, 122, 5209.
- [108] J. Gui, C. Li, Y. Cao, Z. Liu, Y. Shen, W. Huang, X. Tian, *Nano Energy* **2023**, 107, 108155.
- [109] J. Tan, S. Fang, Z. Zhang, J. Yin, L. Li, X. Wang, W. Guo, *Nat. Commun.* **2022**, 13, 3643.
- [110] J. Zhao, R. Ghannam, K. O. Htet, Y. Liu, M. Law, V. A. L. Roy, B. Michel, M. A. Imran, H. Heidari, *Adv. Healthcare Mater.* **2020**, 9, 2000779.
- [111] J. Feng, X. Zhu, Z. Yang, X. Zhang, J. Niu, Z. Wang, S. Zuo, S. Priya, S. (Frank) Liu, D. Yang, *Adv. Mater.* **2018**, 30, 1801418.
- [112] C. Li, S. Cong, Z. Tian, Y. Song, L. Yu, C. Lu, Y. Shao, J. Li, G. Zou, M. H. Rummeli, S. Dou, J. Sun, Z. Liu, *Nano Energy* **2019**, 60, 247.
- [113] J. Dagar, S. Castro-Hermosa, G. Lucarelli, F. Cacialli, T. M. Brown, *Nano Energy* **2018**, 49, 290.
- [114] K. Huang, Y. Peng, Y. Gao, J. Shi, H. Li, X. Mo, H. Huang, Y. Gao, L. Ding, J. Yang, *Adv. Energy Mater.* **2019**, 9, 1901419.
- [115] D. Lv, Q. Jiang, Y. Shang, D. Liu, *npj Flexible Electron.* **2022**, 6, 38.
- [116] M. V. Tholl, H. G. Akarçay, H. Tanner, T. Niederhauser, A. Zurbuchen, M. Frenz, A. Haeberlin, *Appl. Energy* **2020**, 269, 114948.
- [117] K. Song, J. H. Han, T. Lim, N. Kim, S. Shin, J. Kim, H. Choo, S. Jeong, Y.-C. Kim, Z. L. Wang, J. Lee, *Adv. Healthcare Mater.* **2016**, 5, 1572.
- [118] L. Lu, Z. Yang, K. Meacham, C. Cvetkovic, E. A. Corbin, A. Vázquez-Guardado, M. Xue, L. Yin, J. Boroumand, G. Pakeltis, T. Sang, K. J. Yu, D. Chanda, R. Bashir, R. W. Gereau IV, X. Sheng, J. A. Rogers, *Adv. Energy Mater.* **2018**, 8, 1703035.
- [119] G. Apostolou, A. Reinders, M. Verwaal, *Energy Sci. Eng.* **2016**, 4, 69.
- [120] G. Yao, L. Kang, J. Li, Y. Long, H. Wei, C. A. Ferreira, J. J. Jeffery, Y. Lin, W. Cai, X. Wang, *Nat. Commun.* **2018**, 9, 5349.
- [121] J. Gong, B. Xu, X. Guan, Y. Chen, S. Li, J. Feng, *Nano Energy* **2019**, 58, 365.
- [122] Z. Yi, F. Xie, Y. Tian, N. Li, X. Dong, Y. Ma, Y. Huang, Y. Hu, X. Xu, D. Qu, X. Lang, Z. Xu, J. Liu, H. Zhang, B. Yang, *Adv. Funct. Mater.* **2020**, 30, 2000477.
- [123] M. M. Rana, A. A. Khan, G. Huang, N. Mei, R. Saritas, B. Wen, S. Zhang, P. Voss, E. Abdel-Rahman, Z. Leonenko, S. Islam, D. Ban, *ACS Appl. Mater. Interfaces* **2020**, 12, 47503.
- [124] Y. Zhang, L. Wang, L. Zhao, K. Wang, Y. Zheng, Z. Yuan, D. Wang, X. Fu, G. Shen, W. Han, *Adv. Mater.* **2021**, 33, 2007890.
- [125] R. Wang, Z. Du, Z. Xia, J. Liu, P. Li, Z. Wu, Y. Yue, Y. Xiang, J. Meng, D. Liu, W. Xu, X. Tao, G. Tao, B. Su, *Adv. Funct. Mater.* **2022**, 32, 2107682.
- [126] G. Chen, Y. Zhou, Y. Fang, X. Zhao, S. Shen, T. Tat, A. Nashalian, J. Chen, *ACS Nano* **2021**, 15, 20582.
- [127] X. Zhao, Y. Zhou, J. Xu, G. Chen, Y. Fang, T. Tat, X. Xiao, Y. Song, S. Li, J. Chen, *Nat. Commun.* **2021**, 12, 6755.
- [128] J. Xu, T. Tat, X. Zhao, X. Xiao, Y. Zhou, J. Yin, K. Chen, J. Chen, *ACS Nano* **2023**, 17, 3865.
- [129] A. Nozariasbmarz, R. A. Kishore, B. Poudel, U. Saparamadu, W. Li, R. Cruz, S. Priya, *ACS Appl. Mater. Interfaces* **2019**, 11, 40107.
- [130] T. Sun, B. Zhou, Q. Zheng, L. Wang, W. Jiang, G. J. Snyder, *Nat. Commun.* **2020**, 11, 572.
- [131] S. Khan, J. Kim, K. Roh, G. Park, W. Kim, *Nano Energy* **2021**, 87, 106180.
- [132] H. Wang, Y. Sun, T. He, Y. Huang, H. Cheng, C. Li, D. Xie, P. Yang, Y. Zhang, L. Qu, *Nat. Nanotechnol.* **2021**, 16, 811.
- [133] I. Habibagahi, M. Omidbeigi, J. Hadaya, H. Lyu, J. Jang, J. L. Ardell, A. A. Bari, A. Babakhani, *Sci. Rep.* **2022**, 12, 8184.
- [134] P. Chen, P. Wu, X. Wan, Q. Wang, C. Xu, M. Yang, J. Feng, B. Hu, Z. Luo, *Nano Energy* **2021**, 86, 106123.
- [135] M. Etemadzaei, in *Power Electronics Handbook*, (Fourth Edition) (Ed: M. H. Rashid), Butterworth-Heinemann, **2018**, pp. 711–722.
- [136] M. Haerinia, R. Shadid, *Signals* **2020**, 1, 209.
- [137] Y. S. Choi, R. T. Yin, A. Pfenniger, J. Koo, R. Avila, K. Benjamin Lee, S. W. Chen, G. Lee, G. Li, Y. Qiao, A. Murillo-Berlioz, A. Kiss, S. Han, S. M. Lee, C. Li, Z. Xie, Y.-Y. Chen, A. Burrell, B. Geist, H. Jeong, J. Kim, H.-J. Yoon, A. Banks, S.-K. Kang, Z. J. Zhang, C. R. Haney, A. V. Sahakian, D. Johnson, T. Efimova, Y. Huang, et al., *Nat. Biotechnol.* **2021**, 39, 1228.
- [138] V. Sivaji, D. W. Grasse, S. A. Hays, J. E. Bucksot, R. Saini, M. P. Kilgard, R. L. Rennaker, *J. Neurosci. Methods* **2019**, 320, 26.
- [139] A. Adawi, G. Bouattour, M. Ibbini, O. Kanoun, in *2020 17th Int. Multi-Conf. Syst. Signals Devices SSD*, Monastir, Tunisia, **2020**, pp. 156–161.
- [140] C.-C. Kim, Y. Kim, S.-H. Jeong, K. H. Oh, K. T. Nam, J.-Y. Sun, *ACS Nano* **2020**, 14, 11743.
- [141] A. Vázquez-Guardado, Y. Yang, A. J. Bandodkar, J. A. Rogers, *Nat. Neurosci.* **2020**, 23, 1522.
- [142] W. S. Kim, S. Hong, M. Gamero, V. Jeevakumar, C. M. Smithhart, T. J. Price, R. D. Palmiter, C. Campos, S. I. Park, *Nat. Commun.* **2021**, 12, 157.
- [143] V. K. Samineneni, J. Yoon, K. E. Crawford, Y. R. Jeong, K. C. McKenzie, G. Shin, Z. Xie, S. S. Sundaram, Y. Li, M. Y. Yang, J. Kim, D. Wu, Y. Xue, X. Feng, Y. Huang, A. D. Mickle, A. Banks, J. S. Ha, J. P. Golden, J. A. Rogers, R. W. I. Gereau, *PAIN* **2017**, 158, 2108.
- [144] A. Yu, M. Zhu, C. Chen, Y. Li, H. Cui, S. Liu, Q. Zhao, *Adv. Healthcare Mater.* **2024**, 13, 2302460.
- [145] L. Jiang, Y. Yang, Y. Chen, Q. Zhou, *Nano Energy* **2020**, 77, 105131.
- [146] T. R. Nelson, J. B. Fowlkes, J. S. Abramowicz, C. C. Church, *J. Ultrasound Med.* **2009**, 28, 139.
- [147] L. Jiang, Y. Yang, R. Chen, G. Lu, R. Li, D. Li, M. S. Humayun, K. K. Shung, J. Zhu, Y. Chen, Q. Zhou, *Nano Energy* **2019**, 56, 216.
- [148] R. Hinchet, H.-J. Yoon, H. Ryu, M.-K. Kim, E.-K. Choi, D.-S. Kim, S.-W. Kim, *Science* **2019**, 365, 491.
- [149] H. Zhang, P. Gutruf, K. Meacham, M. C. Montana, X. Zhao, A. M. Chiarelli, A. Vázquez-Guardado, A. Norris, L. Lu, Q. Guo, C. Xu, Y. Wu, H. Zhao, X. Ning, W. Bai, I. Kandela, C. R. Haney, D. Chanda, R. W. Gereau, J. A. Rogers, *Sci. Adv.* **2019**, 5, 0873.
- [150] L. Jiang, Y. Yang, R. Chen, G. Lu, R. Li, J. Xing, K. K. Shung, M. S. Humayun, J. Zhu, Y. Chen, Q. Zhou, *Adv. Funct. Mater.* **2019**, 29, 1902522.

- [151] H. Guo, M.-H. Yeh, Y. Zi, Z. Wen, J. Chen, G. Liu, C. Hu, Z. L. Wang, *ACS Nano* **2017**, *11*, 4475.
- [152] X. Pu, W. Hu, Z. L. Wang, *Small* **2018**, *14*, 1702817.
- [153] J. Chen, J. Liang, Y. Zhou, Z. Sha, S. Lim, F. Huang, Z. Han, S. A. Brown, L. Cao, D.-W. Wang, C. H. Wang, *J. Mater. Chem. A* **2021**, *9*, 575.
- [154] H. Nishide, *Science* **2008**, *319*, 737.
- [155] A. Pullanchiyodan, L. Manjakkal, S. Dervin, D. Shakthivel, R. Dahiya, *Adv. Mater. Technol.* **2020**, *5*, 1901107.
- [156] H. Sheng, J. Zhou, B. Li, Y. He, X. Zhang, J. Liang, J. Zhou, Q. Su, E. Xie, W. Lan, K. Wang, C. Yu, *Sci. Adv.* **2021**, *7*, 3097.
- [157] X. Tong, G. Sheng, D. Yang, S. Li, C.-W. Lin, W. Zhang, Z. Chen, C. Wei, X. Yang, F. Shen, Y. Shao, H. Wei, Y. Zhu, J. Sun, R. B. Kaner, Y. Shao, *Mater. Horiz.* **2022**, *9*, 383.
- [158] Q. Lv, X. Li, X. Tian, D. Fu, H. Liu, J. Liu, Y. Song, B. Cai, J. Wang, Q. Su, W. Chen, M. Zou, F. Xiao, S. Wang, Z. Wang, L. Wang, *Adv. Energy Mater.* **2023**, *13*, 2203814.
- [159] C. Gao, C. Bai, J. Gao, Y. Xiao, Y. Han, A. Shaista, Y. Zhao, L. Qu, *J. Mater. Chem. A* **2020**, *8*, 4055.
- [160] L. Manjakkal, A. Pullanchiyodan, N. Yogeswaran, E. S. Hosseini, R. Dahiya, *Adv. Mater.* **2020**, *32*, 1907254.
- [161] N. Hassanzadeh, T. G. Langdon, *J. Mater. Sci.* **2023**, *58*, 13721.
- [162] Y. Zhou, X. Cheng, B. Tynan, Z. Sha, F. Huang, M. S. Islam, J. Zhang, A. N. Rider, L. Dai, D. Chu, D.-W. Wang, Z. Han, C.-H. Wang, *Carbon* **2021**, *184*, 504.
- [163] Y. Liu, H. Zhou, W. Zhou, S. Meng, C. Qi, Z. Liu, T. Kong, *Adv. Energy Mater.* **2021**, *11*, 2101329.
- [164] H. H. Hsu, A. Khosrozadeh, B. Li, G. Luo, M. Xing, W. Zhong, *ACS Sustainable Chem. Eng.* **2019**, *7*, 4766.
- [165] J. Y. Oh, Z. Bao, *Adv. Sci.* **2019**, *6*, 1900186.
- [166] H. H. Hsu, Y. Liu, Y. Wang, B. Li, G. Luo, M. Xing, W. Zhong, *ACS Sustainable Chem. Eng.* **2020**, *8*, 6935.
- [167] J. S. Chae, N.-S. Heo, C. H. Kwak, W.-S. Cho, G. H. Seol, W.-S. Yoon, H.-K. Kim, D. J. Fray, A. T. E. Vilian, Y.-K. Han, Y. S. Huh, K. C. Roh, *Nano Energy* **2017**, *34*, 86.
- [168] J. Yun, Y. Zeng, M. Kim, C. Gao, Y. Kim, L. Lu, T. T.-H. Kim, W. Zhao, T.-H. Bae, S. W. Lee, *Nano Lett.* **2021**, *21*, 1659.
- [169] A. J. Bandodkar, S. P. Lee, I. Huang, W. Li, S. Wang, C.-J. Su, W. J. Jeang, T. Hang, S. Mehta, N. Nyberg, P. Gutruf, J. Choi, J. Koo, J. T. Reeder, R. Tseng, R. Ghaffari, J. A. Rogers, *Nat. Electron.* **2020**, *3*, 554.
- [170] H. J. Sim, C. Choi, D. Y. Lee, H. Kim, J.-H. Yun, J. M. Kim, T. M. Kang, R. Ovalle, R. H. Baughman, C. W. Kee, S. J. Kim, *Nano Energy* **2018**, *47*, 385.
- [171] C. Zhao, Y. Liu, S. Beirne, J. Razal, J. Chen, *Adv. Mater. Technol.* **2018**, *3*, 1800028.
- [172] J. Mohanta, D.-W. Kang, J. S. Cho, S. M. Jeong, J.-K. Kim, *Energy Storage Mater.* **2020**, *28*, 315.
- [173] Q. Wang, C. Zhao, J. Wang, Z. Yao, S. Wang, S. G. H. Kumar, S. Ganapathy, S. Eustace, X. Bai, B. Li, M. Wagemaker, *Nat. Commun.* **2023**, *14*, 440.
- [174] L. Zhou, T.-T. Zuo, C. Y. Kwok, S. Y. Kim, A. Assoud, Q. Zhang, J. Janek, L. F. Nazar, *Nat. Energy* **2022**, *7*, 83.
- [175] W. Ren, C. Ding, X. Fu, Y. Huang, *Energy Storage Mater.* **2021**, *34*, 515.
- [176] P. Li, Z. Jin, L. Peng, F. Zhao, D. Xiao, Y. Jin, G. Yu, *Adv. Mater.* **2018**, *30*, 1800124.
- [177] T. Ye, J. Wang, Y. Jiao, L. Li, E. He, L. Wang, Y. Li, Y. Yun, D. Li, J. Lu, H. Chen, Q. Li, F. Li, R. Gao, H. Peng, Y. Zhang, *Adv. Mater.* **2022**, *34*, 2105120.
- [178] M. H. Lee, J. Lee, S.-K. Jung, D. Kang, M. S. Park, G. D. Cha, K. W. Cho, J.-H. Song, S. Moon, Y. S. Yun, S. J. Kim, Y. W. Lim, D.-H. Kim, K. Kang, *Adv. Mater.* **2021**, *33*, 2004902.
- [179] X. Huang, D. Wang, Z. Yuan, W. Xie, Y. Wu, R. Li, Y. Zhao, D. Luo, L. Cen, B. Chen, H. Wu, H. Xu, X. Sheng, M. Zhang, L. Zhao, L. Yin, *Small* **2018**, *14*, 1800994.
- [180] G. Lee, S.-K. Kang, S. M. Won, P. Gutruf, Y. R. Jeong, J. Koo, S.-S. Lee, J. A. Rogers, J. S. Ha, *Adv. Energy Mater.* **2017**, *7*, 1700157.
- [181] H. Li, C. Zhao, X. Wang, J. Meng, Y. Zou, S. Noreen, L. Zhao, Z. Liu, H. Ouyang, P. Tan, M. Yu, Y. Fan, Z. L. Wang, Z. Li, *Adv. Sci.* **2019**, *6*, 1801625.
- [182] R. K. Pal, S. C. Kundu, V. K. Yadavalli, *ACS Appl. Mater. Interfaces* **2018**, *10*, 9620.
- [183] A. Inman, T. Hryhorchuk, L. Bi, R. (John) Wang, B. Greenspan, T. Tabb, E. M. Gallo, A. VahidMohammadi, G. Dion, A. Danielescu, Y. Gogotsi, *J. Mater. Chem. A* **2023**, *11*, 3514.
- [184] Y. Zhang, S. Zheng, F. Zhou, X. Shi, C. Dong, P. Das, J. Ma, K. Wang, Z.-S. Wu, *Small* **2022**, *18*, 2104506.
- [185] Y. Zhou, X. Cheng, F. Huang, Z. Sha, Z. Han, J. Chen, W. Yang, Y. Yu, J. Zhang, S. Peng, S. Wu, A. Rider, L. Dai, C. H. Wang, *Carbon* **2021**, *172*, 272.
- [186] C. Chen, J. Jiang, W. He, W. Lei, Q. Hao, X. Zhang, *Adv. Funct. Mater.* **2020**, *30*, 1909469.
- [187] E. Alhajji, W. Wang, W. Zhang, H. N. Alshareef, *ACS Appl. Mater. Interfaces* **2020**, *12*, 18833.
- [188] Aaryashree, S. Sahoo, P. Walke, S. K. Nayak, C. S. Rout, D. J. Late, *Nano Res.* **2021**, *14*, 3669.
- [189] S. Mirjalali, A. Mahdavi Varposhti, S. Abrishami, R. Bagherzadeh, M. Asadnia, S. Huang, S. Peng, C.-H. Wang, S. Wu, *Macromol. Mater. Eng.* **2023**, *308*, 2200442.
- [190] J. Tao, Y. Wang, X. Zheng, C. Zhao, X. Jin, W. Wang, T. Lin, *Nano Energy* **2023**, *118*, 108987.
- [191] R. Bagherzadeh, S. Abrishami, A. Shirali, A. R. Rajabzadeh, *Mater. Today Sustainability* **2022**, *20*, 100233.
- [192] C. Zhang, L. Zhou, P. Cheng, X. Yin, D. Liu, X. Li, H. Guo, Z. L. Wang, J. Wang, *Appl. Mater. Today* **2020**, *18*, 100496.
- [193] Y. Zhang, Z. Zhou, L. Sun, Z. Liu, X. Xia, T. H. Tao, *Adv. Mater.* **2018**, *30*, 1805722.
- [194] W. Liu, Z. Wang, G. Wang, G. Liu, J. Chen, X. Pu, Y. Xi, X. Wang, H. Guo, C. Hu, Z. L. Wang, *Nat. Commun.* **2019**, *10*, 1426.
- [195] V. Nguyen, R. Zhu, R. Yang, *Nano Energy* **2015**, *14*, 49.
- [196] Y. Hu, X. Wang, H. Li, H. Li, Z. Li, *Nano Energy* **2020**, *71*, 104640.
- [197] D. Yang, L. Zhang, N. Wang, T. Yu, W. Sun, N. Luo, Y. Feng, W. Liu, D. Wang, *Adv. Funct. Mater.* **2024**, *34*, 2306702.
- [198] Z. Zhang, Q. Zhang, Z. Xia, J. Wang, H. Yao, Q. Shen, H. Yang, *Nano Energy* **2023**, *109*, 108300.
- [199] M. Qu, L. Shen, J. Wang, N. Zhang, Y. Pang, Y. Wu, J. Ge, L. Peng, J. Yang, J. He, *ACS Appl. Nano Mater.* **2022**, *5*, 9840.
- [200] M. Vahdani, S. Mirjalali, M. Chowdary Karlapudi, S. Abolpour Moshizi, J. Kim, S. Huang, M. Asadnia, S. Peng, S. Wu, *Smart Mater. Manuf.* **2023**, *1*, 100016.
- [201] T. Wang, S. Li, X. Tao, Q. Yan, X. Wang, Y. Chen, F. Huang, H. Li, X. Chen, Z. Bian, *Nano Energy* **2022**, *93*, 106787.
- [202] W. Jiang, H. Li, Z. Liu, Z. Li, J. Tian, B. Shi, Y. Zou, H. Ouyang, C. Zhao, L. Zhao, R. Sun, H. Zheng, Y. Fan, Z. L. Wang, Z. Li, *Adv. Mater.* **2018**, *30*, 1801895.
- [203] H. Kang, W. B. Han, S. M. Yang, G.-J. Ko, Y. Ryu, J. H. Lee, J.-W. Shin, T.-M. Jang, K. Rajaram, S. Han, D.-J. Kim, J. H. Lim, C.-H. Eom, A. J. Bandodkar, S.-W. Hwang, *Chem. Eng. J.* **2023**, *475*, 146208.
- [204] G. Jian, S. Zhu, X. Yuan, S. Fu, N. Yang, C. Yan, X. Wang, C.-P. Wong, *NPG Asia Mater.* **2024**, *16*, 12.
- [205] L. Feng, X. Cao, Z. L. Wang, L. Zhang, *Nano Energy* **2024**, *120*, 109068.
- [206] D. Liu, Y. Xing, H. Guo, L. Zhou, X. Li, C. Zhang, J. Wang, Z. Wang, *Sci. Adv.* **2019**, *5*, 6437.

- [207] D. Liu, J.-F. Bao, Y.-L. Chen, G.-K. Li, X.-S. Zhang, *Nano Energy* **2020**, *74*, 104770.
- [208] J. Wang, Y. Li, Z. Xie, Y. Xu, J. Zhou, T. Cheng, H. Zhao, Z. L. Wang, *Adv. Energy Mater.* **2020**, *10*, 1904227.
- [209] S. Bairagi, Shahid-ul-Islam, M. Shahadat, D. M. Mulvihill, W. Ali, *Nano Energy* **2023**, *111*, 108414.
- [210] H. Kabir, H. Kamali Dehghan, S. Mashayekhan, R. Bagherzadeh, M. S. Sorayani Bafqi, *J. Ind. Text.* **2022**, *51*, 4698S.
- [211] Ö. F. Ünsal, A. Ç. Bedeloğlu, *ACS Appl. Nano Mater.* **2023**, *6*, 14656.
- [212] Y. Guo, X.-S. Zhang, Y. Wang, W. Gong, Q. Zhang, H. Wang, J. Brugger, *Nano Energy* **2018**, *48*, 152.



Ziyan Gao is currently a Ph.D. candidate under the supervision of Prof. Chun Hui Wang and Dr. Shuhua Peng in the School of Mechanical and Manufacturing Engineering from the University of New South Wales, Australia. Her research focuses on preparation and application of multifunctional materials for self-powered health monitoring sensors, as well as for energy harvesting and storage.



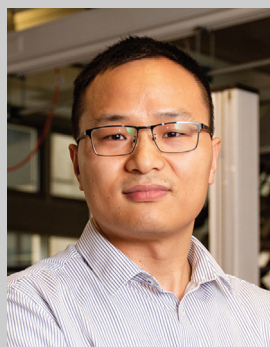
Yang Zhou is currently a research fellow in the School of Mechanical and Manufacturing Engineering, University of New South Wales, Australia since 2018. He obtained his Ph.D. degree from Deakin University in 2018. His research interests focus on the preparation and application of multifunctional composites and wearable energy storage and harvesting devices for various applications.



Jin Zhang is a Scientia Associate Professor and an Australian Research Council Future Fellow at UNSW Sydney. Her current research interests cover functional nanocomposites for energy harvesting and sensing, lightweight structural fiber reinforced composites, 3D printed polymers and composites, etc. She received Endeavour Fellowship from the Department of Industry, Innovation, Science, Research and Tertiary Education, Australia in 2012 and Victoria Fellowship from the Department of Victorian State Development Business and Innovation in 2013. She is leading multiple research projects for sustainable energy, materials and technologies.



Javad Foroughi holds the position of Senior Research Fellow and Chief Investigator within the ARC Research Hub for Connected Sensors for Health at the UNSW. He is also a Visiting Professor at Hanover Medical School in Germany and a recipient of an Australian Research Council DECRA Fellowship. Prof. Foroughi specializes in innovative research in smart materials, focusing on artificial muscles and wearable technology for advanced applications, including medical devices and health monitoring. He is internationally recognized as an emerging leader in the field of smart materials and is widely acknowledged as the inventor of Torsional Carbon Nanotube Artificial Muscles (Science).



Shuhua Peng obtained his Ph.D. degree in polymer science and engineering from Deakin University. He is currently an ARC Future Fellow and Senior Lecturer in School of Mechanical and Manufacturing Engineering at University of New South Wales Sydney. His research covers advanced functional materials for applications such as wearable electronics and sensors, energy harvesting and storage, soft robotics, and advanced manufacturing.



Chun Hui Wang is a Scientia Professor and the Head of School of Mechanical and Manufacturing Engineering at the University of New South Wales (UNSW), Australia. He leads a research team focused on multifunctional composites for extreme environment applications. As the Director of the ARC Research Hub for Connected Sensors for Health, he leads a team of around 60 researchers in developing and deploying wearable sensors for human health monitoring and preventative healthcare.